Coordination Chemistry Reviews 255 (2011) 2764–2784

Contents lists available at ScienceDirect

Coordination Chemistry Reviews

journal homepage: www.elsevier.com/locate/ccr

Review

Nitroxyl (azanone) trapping by metalloporphyrins

Fabio Doctorovich[a,*], Damian Bikiel[a], Juan Pellegrino[a], Sebastián A. Suárez[a], Anna Larsen[c], Marcelo A. Martí[a,b,*]

[a] Departamento de Química Inorgánica, Analítica y Química Física / INQUIMAE-CONICET, Universidad de Buenos Aires, Ciudad Universitaria, Pab. II (1428), Buenos Aires, Argentina
[b] Departamento de Química Biológica, Facultad de Ciencias Exactas y Naturales, Universidad de Buenos Aires, Ciudad Universitaria, Pab. II (1428), Buenos Aires, Argentina
[c] Department of Chemistry, CNS 359, Ithaca College, Ithaca, NY 14850, USA

Contents

Abbreviations: Mb, myoglobin; MbNO, nitrosyl myoglobin; MbO_2, oxymyoglobin; deoxyMb, deoxymyoglobin; metMb, metmyoglobin; Hb, hemoglobin; HbNO, nitrosohemoglobin; Gb, Globin; SOD, superoxide dismutase; CuZnSOD, SOD enzyme with copper and zinc; MnSOD, SOD enzyme with manganese; NOS, NO synthase; P450nor, fungal nitric oxide reductase; RNS, reactive nitrogen species; ROS, reactive oxygen species; HA, hydroxylamine; Por, Porphyrin; TTP, tetratolylporphyrinate; TMPyP, meso-tetrakis(*N*-methylpyridinium-4-yl)porphyrinate; TPPS, meso-(tetrakis(4-sulfonato-phenyl)) porphyrinate; TEPyP, meso-tetrakis (N-ethyl pyridinium-2-yl) porphyrin; MP11, microperoxidase-11; Br_8TPPS, b-octabromo-tetrakis(4-sulfonato-phenyl) porphyrin; Co(P), cobalt 5,10,15,20-tetrakis[3-(p-acetylthio-propoxy)phenyl]-porphyrin; TFPPBr_8, 2, 3, 7, 8, 12, 13, 17, 18-octa-β-bromo-5, 10, 15, 20-tetrakis-(pentafluorophenyl) porphyrin; ORS, oxygen reactive species; NRS, nitrogen reactive species; DBHC, N,O-dibenzoyl-N-hydroxycyanamide; GSH, reduced glutathione; PARP, poly(ADPRibose) polymerase; GAPDH, glyceraldehyde 3-phosphate dehydrogenase; SERCA2a, sarco/endoplasmic reticulum Ca^{2+}-ATPase; DTT, dithiothreitol; sGC, soluble guanylate cyclase; cGMP, guanosine cyclic 3′,5′-monophosphate; AS, Angeliïs salt; PA, Pilotyïs acid; TSHA, toluensulfohydroxamic acid; EPR, electron paramagnetic spectroscopy; NHE, normal hydrogen electrode; SCE, saturated calomel electrode; DFT, density functional theory; EXAFS, extended X-ray absorption fine structure; HPLC, high-performance liquid chromatography.

* Corresponding author. Tel.: +54 11 4576 3378x116; fax: +54 11 4576 3341.
E-mail addresses: doctorovich@qi.fcen.uba.ar (F. Doctorovich), marcelo@qi.fcen.uba.ar (M.A. Martí).

0010-8545/$ – see front matter
doi:10.1016/j.ccr.2011.04.012

ARTICLE INFO

Article history:
Received 4 February 2011
Accepted 26 April 2011
Available online 5 May 2011

Keywords:
HNO
NO
Nitroxyl
Azanone
Nitroxyl anion
Nitrosyl
Iron porphyrin
Heme
Manganese porphyrin
Cobalt porphyrin

ABSTRACT

The present review starts describing nitroxyl (azanone, ^{1}HNO) biological relevance, in relation with NO physiology, from a chemical reactivity perspective. After a description of commonly used azanone donors and their characteristics, the overlapping molecular targets of HNO and NO are presented with an emphasis on heme models and proteins. We present also a brief description of metalloporphyrins and the main characteristics of their nitrosyl complexes, and then describe the reactivity of azanone towards Fe, Ru, Mn and Co porphyrins, briefly mentioning heme proteins, and focusing on ^{1}HNO trapping and its discrimination from NO. A comparison of reaction kinetics and/or nitrosyl product stability with non-heme models is also described. We illustrate the promiscuity of iron porphyrins, the stabilization properties of Ru and the discriminating behavior of Mn and Co porphyrins, which allows the design of optical and electrochemical selective ^{1}HNO sensors. Finally, a comparative analysis and future perspectives are presented, focusing on the *in vivo* reactivity of azanone and its putative endogenous production.

1. Introduction: the chemistry of nitroxyl

1.1. Structure and nomenclature

Nitroxyl, (azanone, HNO), a highly reactive compound is quite an intriguing molecule whose nature has not been completely elucidated so far. Although nowadays it is accepted that singlet ^{1}HNO is the most stable form, triplet ^{3}NOH is also a viable molecule, and both have been observed spectroscopically under rather atypical conditions such as an Argon matrix [1–3]. The energy gap between these species is relatively low, estimated to be only around 20 kcal/mol [4–6].

From the structural viewpoint (see Fig. 1), ^{1}HNO displays a bent structure with the N atom as the central one and an H—N═O angle of about 109°. The N—O bond distance is predicted to be 1.211 Å, which is, as expected, larger than the N—O bond distance in NO due to the addition of electron density to the π antibonding orbital. Due to this fact, the NO infrared stretching frequency for ^{1}HNO is ca. 200 cm^{-1} smaller than for NO.

Apart of the colloquial and widely used name "nitroxyl", HNO has been also known as nitrosyl hydride [8], which does not appear to be appropriate since HNO is a weak acid but definitely not a hydride. According to the Red Book of inorganic nomenclature rules, published by IUPAC in 2005 [10], its compositional name is azanone.[1] This name is derived from the IUPAC name for ammonia (azane) and related to the isoelectronic compound HN═NH (diazene). The other name recommended by IUPAC, based on additive nomenclature, is hydridooxidonitrogen, which has the disadvantage that it also makes reference to a hydride.[2] The main problem with the widely spread name "nitroxyl" is that aminoxyl radicals (of the general formula $R_2NO^{\bullet}$) are usually known as nitroxyl radicals, although there is no close structural relationship among HNO and these organic radicals. Therefore, we suggest the use of the IUPAC name "azanone" for HNO.

The anion of azanone, $^3NO^-$, with a triplet ground state (see below), has been called nitroxyl anion [13], nitroside anion [14], and oxonitrate(1−) [15]. The name suggested in the Red Book is oxidonitrate (1−). There seems to be a lack of consistency in the names suggested by IUPAC, since the acid/base relationship among HNO and NO^- is not represented at all. Considering the above, "azanone anion" seems to be the most appropriate name for NO^-.

1.2. Pharmacology and toxicology of HNO

Intense interest in the biological effects of HNO has emerged mainly due to the wide variety of studies of its closely related sibling nitrogen oxide (NO). Nitrogen oxides, especially NO, play an important role in many physiological processes, specifically in cardiovascular functions where it regulates blood flow, by transmitting the relaxation signal from the endothelium (where NO is produced) to the NO responsive vascular smooth muscle cells [16,17].

Vibrational data (cm^{-1})	
$\nu(NH)_{st}$	2685
$\nu(NO)_{st}$	1565
$\nu(NH)_{bnd}$	1500

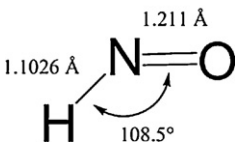

Fig. 1. Structural and vibrational data for ^{1}HNO [7–9].

[1] As proposed by IUPAC, compositional nomenclature is formally based on composition, not structure, and may thus be the (only) choice if little or no structural information is available or a minimum of structural information is to be conveyed [11].

[2] As proposed by IUPAC, additive nomenclature was originally developed for Werner-type coordination compounds, which were regarded as composed of a central atom (or atoms) surrounded by added groups known as ligands, but many other types of compound may also be conveniently given additive names. Such names are constructed by placing the names of the ligands (sometimes modified) as prefixes to the name(s) of the central atom(s) [12].

The almost 20 years of sustained research in the field of nitrogen oxide releasing drugs development has yielded important nitrovasodilators such as NONOates (see below). Interestingly, and in spite of the closely related reactivity of NO and HNO, the biochemical pathways of HNO action have been recently shown to be quite different from those of NO. This understanding was achieved about 10 years ago, when several studies showed clear demonstrations that the presence of NO donors *in vivo* results in different effects than those observed for HNO donors [18].

A number of recent reviews have compared and contrasted both the pharmacology and toxicology of HNO and NO, see for example Wink, Miranda and coworkers [18–20], thus, we will not tackle this subject in depth here, and will outline only briefly the bio-relevance of HNO from a primarily chemical standpoint.

Historically, HNO came into light as a possible biologically active substance in the mid-eighties, in a course of studies related to the anti-alcoholism drug cyanamide (H_2NCN) [21,22]. Cyanamide generates HNO in an oxidative reaction (with catalases or peroxidases) [23], which in turn would inhibit the enzyme aldehyde dehydrogenase. This last inhibition step proceeded via reaction at the cysteine thiolate active site residue by the released HNO, and was thus one of the first evidences indicating a high reactivity of ^{1}HNO for thiolates (RS^-) [24,25]. Later, other examples of HNO targeting reactive thiolates have been reported with cysteine protease, where it inhibits cathepsin B functionality, as well as with yeast copper-thiolate transcription factor protein [23–25].

Another biological key feature of HNO reactivity is its high reactivity for ferric and ferrous heme proteins, which will be discussed in subsequent sections. Also interestingly, HNO is able to react with other metalloproteins such as CuZnSOD and MnSOD [18,26].

From the physiological viewpoint, HNO is known to cause a vasorelaxation response as shown in several studies. HNO donors such as Angeli's salt and cyanamide act in a fashion similar to that of NO [27,28]. However, the difference between the effects of HNO donors and NO, is that the former shows preferential venous dilation while the latter tends to affect arterial and venous sides [19]. HNO donors also cause an increase in cardiac muscle contractility, via a combined positive effect on the force related with muscle contraction, with simultaneous relaxation of the cardiac muscles (inotropic and lusitropic effects, respectively), resulting in increased cardiac output. A number of studies have been reported where several models are proposed in order to explain the mechanism of ^{1}HNO effect on the cardio-vascular system. For example, HNO targets a critical cysteine residue in sarco/endoplasmic reticulum Ca^{2+}-ATPase (cysteine 674 in SERCA2a) [29]. It has also been shown, that HNO modifies critical thiols in phosphorylating phospholamban (PLN) and increases SERCA2a activity by removing an inhibition of the Ca^{2+} pump [30]. In summary, to the present date, a significant body of evidence has been collected pointing to possible positive effects of HNO in preventing heart failure, by acting on various potential targets via diverse mechanisms. This is a strong incentive for the development of new HNO donors for pharmacological applications.

Another therapeutic application of HNO may stem from the finding that it may be a powerful preconditioning agent that helps to alleviate the negative consequences of an ischemic event and reperfusion injury, characterized by blood flow deprivation followed by hypoxia and eventual heart tissue necrosis. The corresponding studies show that a dramatic decrease in the infarct size was achieved by pre-treating heart tissues with Angeli's salt, (the most common HNO donor). However, it has been shown that HNO simultaneously increases the infarction size if administered during an ischemic event. In this case, the pharmacological effect of NO is drastically different from that of HNO, since NO was has protective properties in cardiac ischemia reperfusion injuries when given during the reperfusion phase [31]. Finally, HNO pro-drugs may also be effective as anticancer agents, as HNO irreversibly hampers activity of glyceraldehyde 3-phosphate dehydrogenase (GAPDH)—a critical enzyme in glycolysis, which most solid tumors utilize as their energy source. Also, studies show that breast cancer cells are affected by Angeli's salt presence via its inhibitive interaction with poly(ADPRibose) polymerase (PARP). PARP function is considered critical in DNA repair process, and thus ability to inhibit PARP may potentially furnish an effective approach to disruption of cancer cell reproduction [32]. In summary, HNO releasing agents have interesting perspectives as potential therapeutic compounds. However, more work is needed to understand the chemical mechanisms underlying the observed physiological effects.

1.3. HNO production in vivo

A key question related with HNO and its biological role, concerns the possibility of in vivo endogenous formation of HNO. The studies at this time are contradictory and a definite answer is still missing. The most accepted pathway for *in vivo* HNO production has been speculated to result from the enzymatic activity of nitric oxide synthase (NOS) under particular cofactor conditions [33–35]. In the proposed reaction, the substrate arginine is reduced by six electrons to yield HNO according to the following reaction 1:

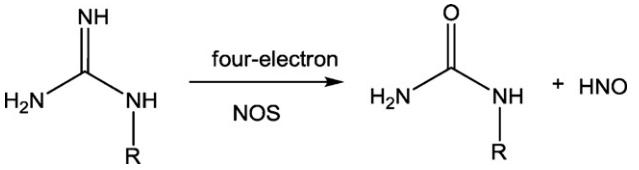

(1)

In the corresponding studies and based on N_2O and NH_2OH detection, the authors suggested that the product from NOS enzymatic turnover in the absence of the cofactor biopterin, should be HNO and not NO [34,36]. Additional evidence for endogenous HNO generation included detection of Fe(II)—NO coordination in NOS, rather than the usual ferric resting state [34,37]. Very recently, Marletta and coworkers argued that in the last step of NO production by NOS, a biopterin centered radical oxidizes the $\{FeNO\}^7$ to an $\{FeNO\}^6$ species, and then NO is released from the ferric iron. It remains however to be proven and seems unlikely that the $\{FeNO\}^7$ intermediate can actually release $^3NO^-$ or ^{1}HNO [38,39]. Although these and other results have been presented as evidence for HNO intermediacy in NOS metabolism, the HNO production mechanism has not been established conclusively and the results remain open to interpretation.

Another endogenous HNO source, relies on the oxidation of hydroxylamine (HA), or other alcohol amine, such as hydroxyurea or N-hydroxy arginine. *In vivo* such a process is postulated to depend on the activity of several heme proteins, which are able to stabilize oxo-ferryl species, (compound I and compound II), like peroxidases [26,40,41]. Recently, Donzelli et al. evaluated ^{1}HNO production by this mechanism [42], with a newly developed selective assay in which the reaction products, $GS(O)NH_2$, in the presence of reduced glutathione (GSH) are quantified by HPLC. Their results showed that metmyoglobin, horseradish peroxidase and mieloperoxidase where efficient HNO producers using hydroxylamine as a substrate. Other peroxidases and catalases are able to oxidize *in vitro* N-containing substrates with lower nitrogen oxidation states such as hydroxylamine, hydroxyurea, hydroxamic acid, azide and cyanamide, with the concomitant production of HNO as recently reviewed by King and coworkers [23]. However, there are several remaining unresolved questions concerning the proposed mechanism (which is outlined below, reaction 2).

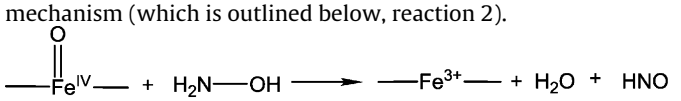

(2)

For example, one point of debate concerns whether the generated HNO molecule may escape from the ferric heme pocket, which seems unlikely given the HNO reactivity towards ferric hemes. Also important is the way in which the protein is driven to the formation of the oxo-ferryl species *in vivo*, which *in vitro* was performed by the addition of H_2O_2 [42–45].

In the case of porphyrin models [46], it was proposed that for $[Fe^{III}(TPPS)]^{3+}$ the formation of HNO from hydroxylamine occurred by a two-electron *trans*-disproportionation of a bis-coordinated NH_2OH complex producing a low spin ferric intermediate $[Fe^{III}(Por)(NH_3)(HNO)]$. Based on the experimental kinetic evidence, and the obtained N_2/N_2O ratios from the reaction mixtures, a different mechanism was proposed for Fe^{III}MP11, in which the formation of $[Fe^{III}(Por)(NHis)(HNO)]$ was suggested to result from the reaction of free HA towards iron bound HA.

Another suggested endogenous source of azanone stems from the reduction of NO to HNO by Mn or Fe superoxide dismutases [43,47] or by xanthine oxidase (XO) [42]. Although both types of enzymes have been reported as capable of HNO production, the corresponding studies relied on indirect methods for HNO detection which are sometimes difficult to interpret or unreliable.

Finally, there is at least one non-enzymatic proposed route for endogenous HNO production, which follows the decomposition of nitrosothiols (RSNOs) by other thiols (such as glutathione) according to the reaction 3 shown below:

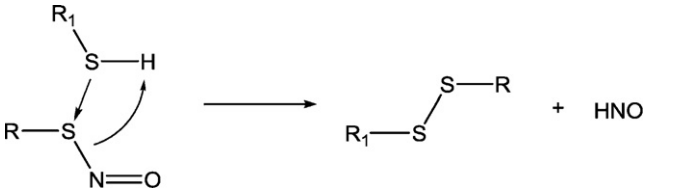

(3)

Although this mechanism has not been established for an *in vivo* process, *in vitro* studies show that the reactivity of excess thiol with RSNOs leads to disulfide and HNO formation [48,49]. Moreover, HNO is also generated from the nitrosation of dithiol compounds such as dithiothreitol (DTT) and lipoic acid [42].

Last but not least, it should be stressed that none of the mechanisms described above have been undoubtedly confirmed, primarily due to the difficulties with the unequivocal detection of HNO. Currently, the formation of N_2O, NH_2OH, or ferrous nitrosyl species is used as indirect evidence of HNO production, but clearly the development of reliable analytical methods for quantitative HNO detection is in high demand for the advancement of biomedical research in this area.

To summarize, HNO appears to have promising biochemical prospects. Three areas are emerging with regard to the potential biomedical applications of HNO releasing molecules as therapeutic agents: cardiovascular therapy, reperfusion injury-preventive therapy, and anti-cancer treatment. On the other hand, endogenous *in vivo* HNO production still remains as an interesting hypothesis that needs to be proved or rejected.

1.4. HNO donors

^{1}HNO and $^3NO^-$ are, as will be shown in next chapters, very reactive molecules. One of the key reactions is ^{1}HNO reaction with itself (i.e. dimerization) to yield water and N_2O at nearly diffusional speed. Therefore, nitroxyl solutions are not stable and HNO, if not produced continuously, is readily lost. In addition, HNO cannot be isolated in the solid state, $^3NO^-$ is even more unstable, and its reactivity is less understood. To overcome these problems, working with ^{1}HNO (or $^3NO^-$) has always relied on the use of azanone donor molecules, i.e. compounds that under certain specific conditions spontaneously release ^{1}HNO or $^3NO^-$.

A number of reviews, tackling the subject of ^{1}HNO or $^3NO^-$ generation have appeared over the past decade. Specifically, we recommend two reviews published in 2005 by Miranda et al. [50,51], which include a deep description of the donors reactivity. Hence, here we will only briefly outline the key methods of HNO generation and refer the reader to the above reviews for further information and original references, and cite explicitly only more recent publications.

1.4.1. Angeli's salt

Historically, the first method for *in situ* generation of HNO was described by Angeli in 1896, from decomposition of $Na_2N_2O_3$ [52,53]. Angeli's salt (AS) is still routinely used for this purpose. The generally accepted mechanism for spontaneous decomposition of AS to yield HNO and nitrite, involves monoprotonation of Angeli's salt anion between pH 4 and 8, as shown below (Reaction 4) [44,50,54].

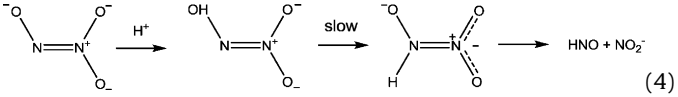

(4)

In strongly acidic media, (i.e. below pH 3), the main nitrogen containing product of the decomposition of Angeli's salt is NO (and not HNO) [55]. Equation 5 below describes the sequence of proposed events leading to NO formation via an oxygen-diprotonated species:

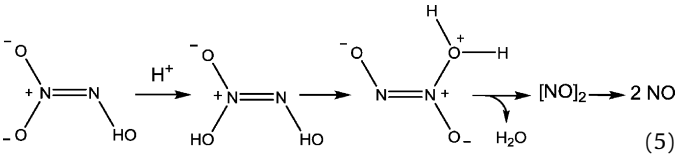

(5)

The close comparison of the experimentally determined and calculated rate constants values for the above equations supports the plausibility of this mechanism [54] NO can also be generated in a direct redox process with hexaammineruthenium(III) or hexacyanoferrate(III) in basic media.

In summary, Angeli's salt is commonly regarded as a reliable HNO donor in near-neutral media, with a pH-dependent and first-order thermal decomposition. From pH 4 to 8 the rate constant is practically invariable, being $6.8 \times 10^{-4}\ s^{-1}$ at 25 °C, equivalent to a half-life of 17 min [50,52–55] (correspondingly, this value is $5 \times 10^{-3}\ s^{-1}$ at 37 °C, equivalent to ~2 min half-life) [58].

1.4.2. Piloty's acid

The second method of significance is generation of HNO from an organic compound [60–64], Piloty's acid (PA), via heterolysis in basic medium, according to the equation 6 shown below [65,66]:

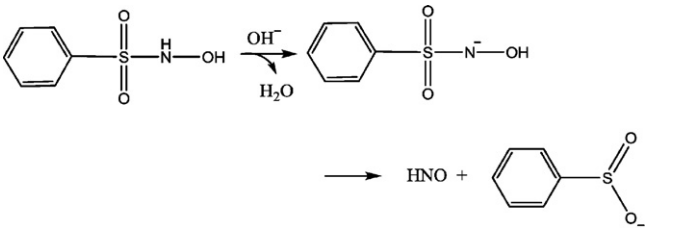

(6)

The reaction is spontaneous once the sulfohydroxamic moiety is deprotonated. Therefore, PA will spontaneously and continuously produce HNO above certain pH, which is related to the corresponding pK_a. Several PA derivatives have been synthesized recently [64],

such as the *p*-nitro; 2,4,6-triisopropyl; *p*-methoxy and other derivatives. These compounds also produce HNO and start to decompose at pH values as low as 2, therefore covering, as HNO donors, most of the pH range [Doctorovich, F., private communication].

The rate constants for decomposition of Piloty's acid at pH 13 and Angeli's salt at pH 4–8 are comparable, with the values for both falling in the 10^{-3} to 10^{-4} s^{-1} range (at 25–35 °C). Similar to AS in neutral and slightly acidic range, PA under basic conditions exhibits half-lives on the order of minutes (27 min at 25 °C and 6 min at 35 °C) [66,67]. All PA derivatives show similar decomposition rates, although at different pH ranges [Doctorovich, F., private communication]. One possible complication with Piloty's acid stems from its easy oxidation under aerobic conditions—according to the equation 7 below, resulting in generation of NO instead of ^{1}HNO:

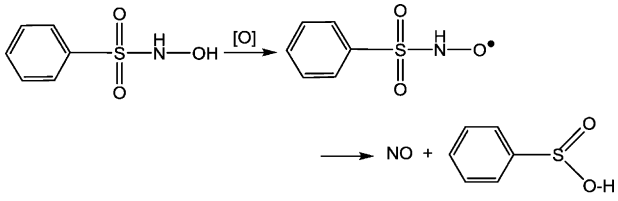

(7)

The above process is predominant under typical physiological conditions (aerobic and near neutral pH), where generation of HNO becomes significantly slower [68].

Other characterized HNO donors of this class are hydroxylamine-*N*-sulfonic acid ($HOSO_2NHOH$) and *N*-hydroxymethanesulfonamide (methanesulfohydroxamic acid (MSHA), methylsulfonyl hydroxylamine; CH_3SO_2NHOH), see reaction (8):

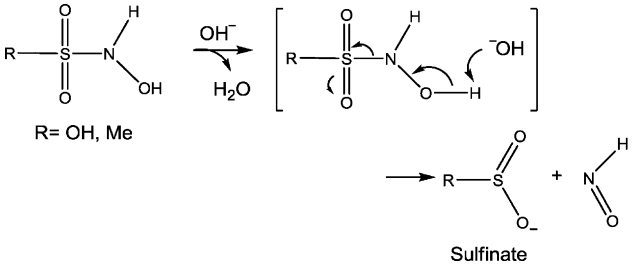

(8)

Both Piloty's acid and Angeli's salt are still widely used for generation of HNO for pharmacological studies. Of the two, Angeli's salt has a comparative advantage of reliable generation of HNO under oxidative aerobic conditions and in neutral pH, as opposed to Piloty's acids giving off NO as main product in this case. However, the structure of Angeli's salt anion is not amenable to derivatization. Hence, there is less flexibility in tailoring the function of HNO delivery for specific biomolecular targets.

1.4.3. NONOates (diazenium diolates)

NONOates (diazenium diolates) are a class of compounds related to Angeli's salt, which release HNO according to the general equation 9 shown below [69]:

$$[RNH{-}N(O){=}NO]^- \rightleftharpoons [RN{=}N(O){-}NHO]^- \rightarrow HNO + RNNO^- \quad (9)$$

There have been also investigations reported for the photoinduced decomposition of NONOates by laser kinetic spectroscopy, specifically for diazen-1-ium-1,2,2-triolate (Angeli's anion) and (*Z*)-1[*N*-(3-aminopropyl)-*N*-(3-aminopropyl)amino]diazen-1-ium-1,2-diolate (DPTA NONOate, shown below in Compound #1). The analyzed distributions of the primary flash photolysis products showed that neither diazeniumdiolate is a highly selective photochemical generator of azanone or nitric oxide [70].

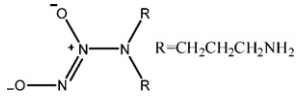

Several publications report the use of secondary alkyl-amines for the successful production of HNO [71]. There is also reported example for HNO generation at neutral pH from a NONOate derivative with primary isopropyl amine [49].

1.4.4. Cyanamide

In biomedical context, during the investigation of the metabolism of alcohol deterrent cyanamide, HNO generation was detected as one of the byproducts of the mitochondrial enzyme catalase functioning in peroxidative mode. The reaction is thought to occur according to the equation 10 shown below [25]:

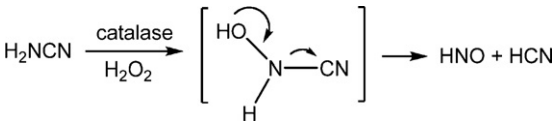

(10)

HCN generation was detected directly in this enzymatically activated process, and HNO formation was initially only postulated. Later, nitroxyl generation was supported by N-15 and C-13 labeling studies. Although clearly cyanamide cannot be thought as a spontaneous HNO donor, production of HNO and HCN by catalase could occur *in vivo* if conditions are satisfactory [72].

Numerous HNO releasing prodrugs are currently being developed, in pursuit of the stabilization of N-hydroxycyanamide, via *N,O-bis*-acylation. One of these prodrugs *N,O*-dibenzoyl-*N*-hydroxycyanamide (DBHC) was synthesized and is in fact a potent inhibitor of acetaldehyde enzymatic oxidation in yeast. DBHC exhibits HNO–releasing behavior similar to that of cyanamide – according to the reaction 11 below.

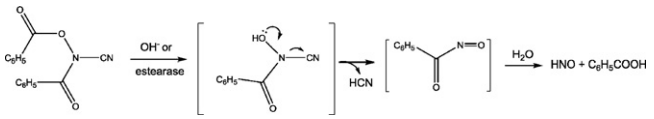

(11)

1.4.5. Hydroxylamine and related compounds

A general strategy of employing hydroxylamine, or its' substituted version with a good leaving group on N atom has also been discussed in terms of its' potential for HNO generation, according to the general equation 12 shown below:

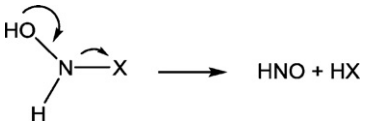

(12)

For example, the production of HNO from dehydrogenation of *N*-acylhydroxylamines has been documented and the investigation showed that periodate oxidation of benzohydroxamic acid produced benzoic acid and N_2O, derived presumably from HNO, according to the reaction 13 below:

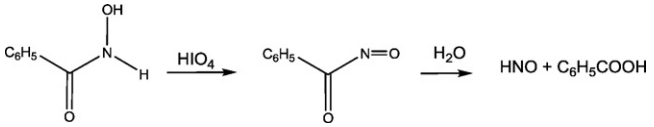

(13)

In addition, King and collaborators [73] achieved HNO generation by oxidation of hydroxyurea with periodate via the carbamylnitroxyl intermediate (Eq. 14).

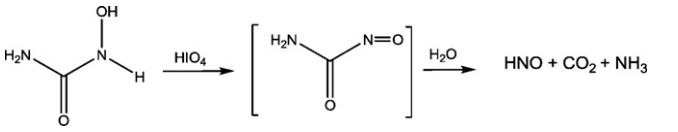

(14)

Consequently, hydroxyurea is one of the two clinically approved bioactivated HNO donors (along with Pilotyĭs acid, vide infra). However, it should not be overlooked that hydroxyurea can also generate NO under certain conditions *in vivo* through catalase-mediated oxidation [74].

1.4.6. Acyloxy nitroso compounds

In 2006, King and coworkers also reported synthesis and hydrolysis of *acyloxy nitroso compounds* to yield HNO according to the equation 15 below [75]:

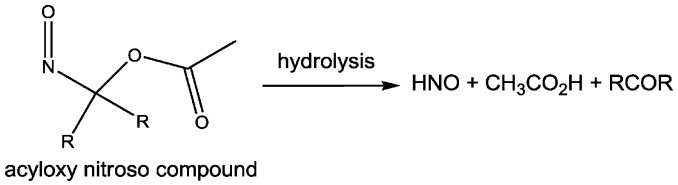

(15)

The HNO releasing ability of these compounds was studied by spectroscopic methods (chemiluminescence and gas chromatography) and estimated in chemical and bio-essays. Hydrolysis of these compounds produces nitrous oxide, the dimerization and dehydration product of HNO, which provides evidence for the intermediacy of HNO. The rate of hydrolysis in the above reaction depends on pH and the structure of the acyl group of the acyloxy nitroso compound. Two compounds – 1-nitrosocyclohexyl trifluoroacetate and 1-nitrosocyclohexyl acetate – relax a pre-constricted rat aortic ring in a fashion comparable to that of Angeli's salt. Thus, acyloxy nitroso compounds represent a new class of HNO donors that may provide a viable alternative to Angeli's salt and Piloty's acid for biological systems.

Benzohydroxamic acid can be dehydrogenated by the azodicarboxamide to benzoylnitroxyl, which solvolyzes to give HNO (Eq. 16). The same reagent can also be used to dehydrogenate the aliphatic *N*-*t*-butyloxycarbonylhydroxylamine to form an HNO-generating nitrosocarbonyl intermediate. In both cases, HNO is invoked as an intermediate based on N_2O detection [76].

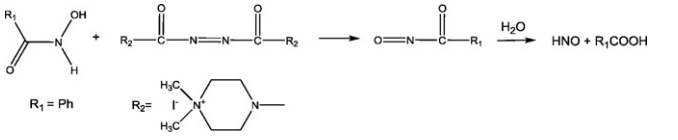

(16)

Recently a number of other acyl nitroso compounds have been synthesized by Miyata and coworkers to generate HNO via retro Diels-Alder reactions [77]. In a very recent example, HNO release from one such compound has been achieved in a controllable fashion upon photo-induction [78], with the change of the solvent polarity in this case controlling the selective generation of NO versus HNO, according to Scheme 1 shown below.

In summary, we concur with the conclusions of the previous reviewers of this field, that in spite of a multitude and variety of available HNO donors, many of them have several and important limitations. The interest of the HNO potential for biomedical applications is very high, and thus active research in this area is bound to produce new viable HNO donor pathways flexible enough to be correlated with specific targets for HNO delivery. Table 1 summarizes all the abovementioned HNO donors.

1.5. Reactions of HNO and NO with biologically relevant small molecules

In a relatively recent review by Miranda [51], the fundamental chemistry of ^{1}HNO and $^3NO^-$ has been described in a careful and exhaustive manner. We will briefly describe its chemistry, make note of new advances regarding this topic, and focus on the comparison with NO reactivity. Rate constants and some reduction potentials for the reactions mentioned below are summarized in Table 2.

1.5.1. Spin states and acidity

While NO is a free radical with a doublet ground state, ^{1}HNO has a singlet ground state [87,88]. It is a weak acid with an accepted pK_a of 11.4 [79,89]. Interestingly enough, its anion, $^3NO^-$, has a triplet ground state [90–93], the same as the isoelectronic O_2 molecule. Therefore, loss of a proton from HNO is not a simple acid/base equilibrium but a spin-forbidden slow deprotonation (Table 2, Eq. 17) [79]:

$$^1HNO + OH^- \rightleftharpoons {}^3NO^- + H_2O \quad (17)$$

Reprotonation of $^3NO^-$ to ^{1}HNO is also slow (Table 2). In principle, coordination should lower the pK_a of HNO. In agreement with this assumption, Olabe and coworkers have reported that the complex $[Fe(II)(CN)_5(HNO)]^{3-}$ has a pK_a value of 7.7 [94]. However, Farmer and coworkers have suggested that the pK_a value for the HNO-Fe(II)Mb adduct is close to 11, probably due to the effect of hydrogen-bonding interactions in the vicinity of the active site [95]. NO acts as base by coordinating to a large variety of metal centers, and many nitrosyl complexes are known [96], with NO+, NO$^\bullet$ or NO^- character (see chapter 2.1). Its redox partner NO^+ is on the other hand, a strong electrophile and acid.

1.5.2. Dimerization

HNO dimerizes with a second order rate constant of ca. 10^7 to produce hyponitrous acid which finally decomposes to produce nitrous oxide (Table 2, Eq. 18) [79,97,98].

$$2HNO \rightarrow HONNOH \rightarrow N_2O + H_2O \quad (18)$$

Between pH 7.5 and 10.5, where the species $HN_2O_2^-$ accounts for most of the hyponitrous acid in solution (pK_a = 10.9), its decomposition rate exhibits a plateau with k (25°) = 5.0×10^{-4} s^{-1} (half-life 23 min) [80]. Outside this pH range the decomposition rate becomes even slower up to values of around 10^{-6} s^{-1}. Below pH 5, and in the absence of radical scavengers hyponitrous acid can decompose by a radical chain mechanism producing N_2 and NO_3^- [99], so it has to be taken into account that below pH 5 ethanol or other radical scavengers should be added to the reaction mixtures to avoid complications arising from the radical chain mechanism.

Regarding $^3NO^-$, although it has been suggested that to dimerize with $k > 8 \times 10^6$ M^{-1} s^{-1} [51], there is no experimental evidence to support this asseveration. According to Bonner and coworkers, "Coulomb barrier considerations lead one to expect inhibition of the dimerization reaction with increasing deprotonation of HNO" [100]. However, it has been recently reported by Lymar and coworkers that the spin forbidden reaction of $^3NO^-$ and ^{1}HNO takes place with a rate constant of 6.6×10^9 M^{-1} s^{-1} (Eq. 19) [70].

$$^3NO^- + {}^1HNO \rightarrow N_2O + OH^- \quad (19)$$

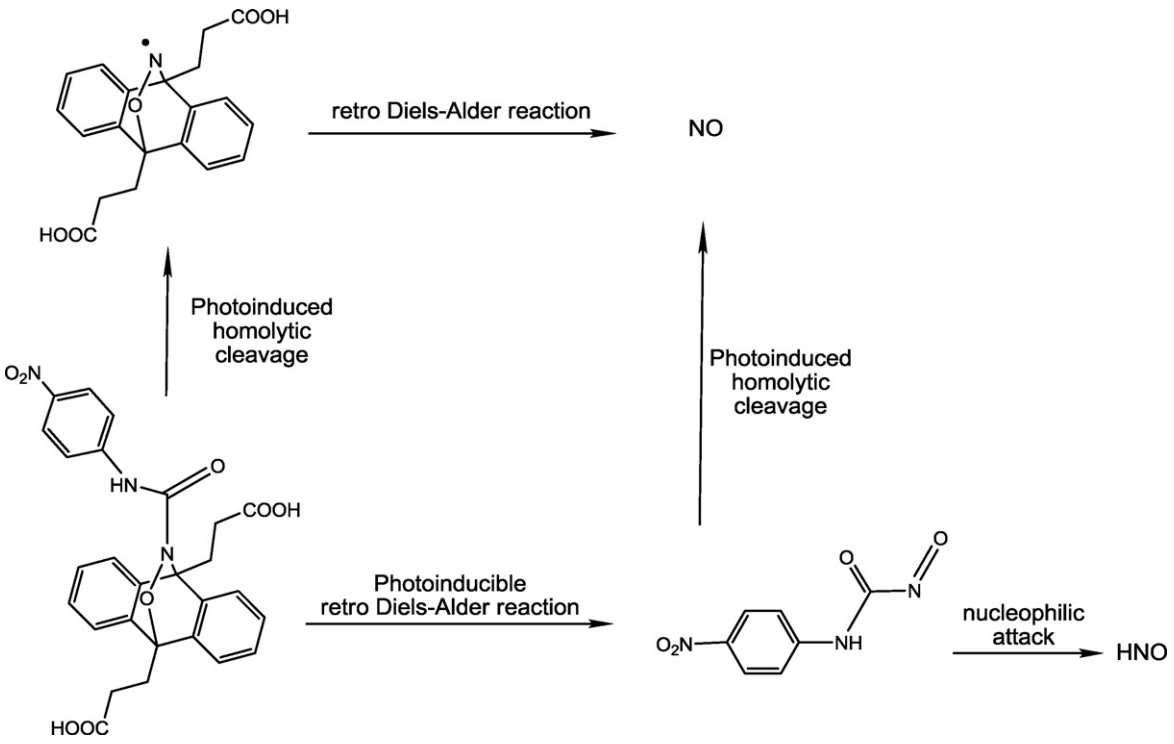

Scheme 1. Selective generation of HNO and NO by photo-induced cleavage of an acyl nitroso compound [77,78].

This result is based on indirect kinetic observations. On the other hand, it is a surprising fact – even for the authors – that a spin forbidden reaction would be so fast; according to Lymar this could be due to the very large driving force for this reaction (with an estimated ΔG of −80 kcal/mol). Although $^3NO^-$ is isoelectronic with O_2, due to its negative charge is expected to be more nucleophilic, so reaction 19 could be thought as a nucleophilic addition of nitroxyl anion to the N atom of ^1HNO to produce the intermediate $HONNO^-$ (after electronic rearrangement and a 1,2 H shift), which decomposes to produce N_2O (ec. 20). In principle, $^1HN{=}O$ could be expected to suffer this type of nucleophilic attack in a similar way to carbonyl ($R_2C{=}O$) compounds. However, this particular reaction is complicated by the different spin states of azanone. Possibly, further theoretical studies are needed to understand the reaction details. On the other hand and unlike ^1HNO, NO has little tendency to dimerize to $(NO)_2$ with a small equilibrium constant $K = 8.360 \times 10^{-2}$ (120 K), and therefore is rather stable in solution [101].

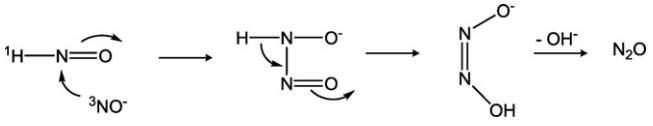

(20)

1.5.3. Oxidation

The reaction of ^1HNO with O_2, which has been studied in the gas phase [102] is rather slow, due to their different spin states, $k \approx 10^3\ M^{-1}\ s^{-1}$ (see Table 2). Strikingly, the reaction product is still unknown although it has been proposed that the reaction proceeds through Eq. 21, leading to NO and a radical hydroperoxy species [79].

$$^1HNO + O_2 \rightarrow NO^{\bullet} + HO_2^{\bullet} \quad (21)$$

On the other hand, $^3NO^-$ reacts with O_2 at a second-order rate to produce peroxynitrite (Eq. 24) [79].

$$^3NO^- + O_2 \rightarrow ONOO^- \quad (22)$$

in a reaction isoelectronic with the also second-order reaction 25 [51,82,83].

$$NO + O_2^- \rightarrow ONOO^- \quad (23)$$

NO, on the contrary, reacts with O_2 following third-order kinetics, and at a slower rate. The mechanism of this reaction is shown in a simplified manner in Eqs. 24–26 [84].

$$2NO + O_2 \rightarrow\rightarrow\rightarrow 2NO_2 \quad (24)$$

$$NO_2 + NO \rightarrow N_2O_3 \quad (25)$$

$$N_2O_3 + H_2O \rightarrow 2NO_2^- + 2H^+ \quad (26)$$

1.5.4. Reactivity towards NO

The accepted standard reduction potential for the $NO/^3NO^-$ couple is −0.8 V [89]. At physiological pH ^1HNO is expected to be the main nitroxyl-related species, and it has an estimated $E^\circ(NO,H^+/^1HNO) \approx -0.14$ V, becoming −0.55 V at pH 7 (all values against NHE) [79]. As a result, it is currently under discussion if NO could be reduced to $^3NO^-$ or ^1HNO in mammalian systems since on one hand the reduction potentials mentioned above (−0.8 and −0.55 V) are in the limit of biological reducing agents, and other species which are present in higher concentrations, such as O_2, are more favorable to be reduced. On the contrary, $^3NO^-$ should function as a strong reducing agent yielding NO, while ^1HNO usually acts as an electrophile, as mentioned for reaction 19.

Last but not least, both $^3NO^-$ and ^1HNO react with NO, with quite distinct second-order rate constants which differ in three orders of magnitude favoring reaction with $^3NO^-$ (Table 2, Eqs. 27 and 28) [81]:

$$^3NO^- + NO \rightarrow N_2O_2^- \quad (27)$$

$$^1HNO + NO \rightarrow N_2O_2^- + H^+ \quad (28)$$

The resulting $N_2O_2^-$ radical extremely rapidly acquires another NO molecule, producing the closed shell $N_3O_3^-$ anion, which

Table 1
HNO donors.

Parent donor name	Structure	Product after HNO release	Mechanism of HNO release	Ref.
Angeli's salt	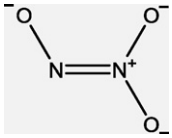	NO_2^-	Protonation (pH 4–8, aq.)	[54,56–59]
Piloty's acid (Aromatic sulfo-hydroxamic acid)	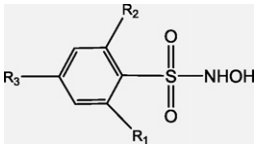	$ArSO_2H$	Deprotonation (pH 2–14, aq. or organic solvents)	[66,67]
Aliphatic sulfo-hydroxamic acid	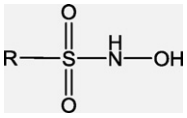	RSO_2H	Deprotonation	[66,67]
NONOates (diazeniumdiolates)	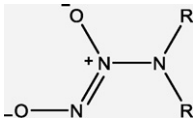	$RN=NO^-$	Thermal	[69,71]
Cyanamide	R_2NCN	HCN	Enzymatic	[72]
Hydroxylamine	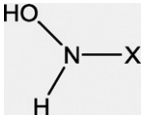	HX	Oxidative (HIO_4)	[73]
Acyloxy nitroso	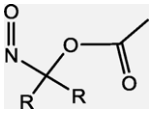	$CH_3COOH + RC(O)R$	Hydrolytic	[75]
Acyl nitroso	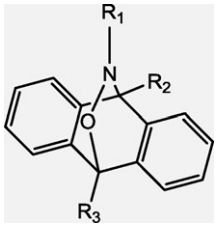	R_1COOH	Photochemical	[77,78]

Table 2
Rate constants and reduction potentials for reactions of azanone, azanone anion and nitric oxide with biologically relevant small molecules.

Eq. #	Reaction	Rate constant[a]	Reference
17	$^1HNO + OH^- \rightarrow {}^3NO^- + H_2O$	$4.9 \times 10^4\ M^{-1}\ s^{-1}$	[67]
18	$^1HNO + {}^1HNO \rightarrow HONNOH$	$8 \times 10^6\ M^{-1}\ s^{-1}$	[79]
	$HONNOH \rightarrow N_2O + H_2O$	$5.0 \times 10^{-4}\ s^{-1}$	[80]
21	$^1HNO + O_2 \rightarrow NO + HO_2$ (?)	$3–8 \times 10^3\ M^{-1}\ s^{-1}$	[18,26,79]
28	$^1HNO + NO \rightarrow N_2O_2^- + H^+$	$5.8 \times 10^6\ M^{-1}\ s^{-1}$	[81]
-17	$^3NO^- + H_2O \rightarrow {}^1HNO + OH^-$	$1.2 \times 10^2\ s^{-1}$	[79]
19	$^3NO^- + {}^1HNO \rightarrow N_2O + OH^-$	$6.6 \times 10^9\ M^{-1}\ s^{-1}$	[70]
22	$^3NO^- + O_2 \rightarrow ONOO^-$	$2.7 \times 10^9\ M^{-1}\ s^{-1}$	[79]
27	$^3NO^- + NO \rightarrow N_2O_2^-$	$3.0 \times 10^9\ M^{-1}\ s^{-1}$	[81]
23	$NO + O_2^- \rightarrow ONOO^-$	$4\text{-}7 \times 10^9\ M^{-1}\ s^{-1}$	[82,83]
24	$2NO + O_2 \rightarrow 2NO_2$	$2.54 \times 10^6\ M^{-2}\ s^{-1}$	[84]

	Potential vs NHE	Reference
$NO + H^+ + e^- \rightarrow {}^1HNO$	$E^\circ \approx -0.14$ V	[85]
$NO + e^- \rightarrow {}^3NO^-$	$E^\circ < -0.8$ V	[86]

[a] Rate constants are given at room temperature and pH 7.

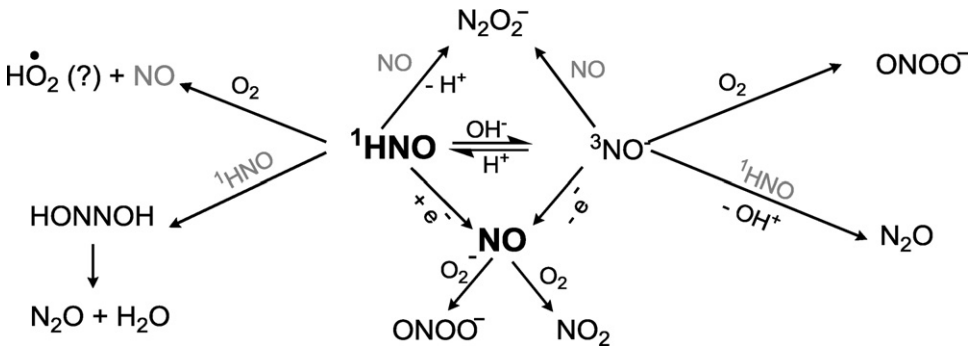

Scheme 2. Reactions of Nitroxyl and Nitric Oxide [18,26,67,70,79–86].

decays to the final products $N_2O + NO_2^-$ with a rate constant of ca. $300\,s^{-1}$.

A summary of the reactions of NO and HNO/NO^- with small molecules is shown in Scheme 2.

2. Azanone reactivity towards metalloporphyrins

2.1. Metalloporphyrin nitrosyl complexes of Mn, Fe and Co

Besides the small molecules, described above, the main targets of NO and HNO in biological systems are thiols [51,103], and metalloproteins, principally heme proteins [104,105]. In this context, much of the knowledge about the reaction of NO with hemes comes from the study of its reactivity with isolated heme models, id est., metalloporphyrins, mainly of iron, but also manganese, cobalt and ruthenium [106]. There are two salient issues about metalloporphyrin nitrosyl complexes. The first concerns their formation and dissociation rates, the second is related to the NO geometry and its effect on other *trans* ligands. Usually NO binds to the metal via the nitrogen atom, and its character ranges (formally) from that of NO^+ to that of NO^- [104,107]. A good and useful description of the metal-NO moieties was originally presented by Enemark and Feltham in the 70 s [108–110], and is depicted as $\{MNO\}^n$, where M is the corresponding metal center, and the key parameter is the number *n*, corresponding to the sum of the metal *d* electrons plus the nitrosyl π^* electrons.

Accordingly, for example $\{FeNO\}^6$ complexes correspond to ferric nitrosyls, displaying NO^+ character, a linear Fe–N–O geometry and NO stretching mode $\upsilon_{NO} \approx 1937\,cm^{-1}$, while $\{FeNO\}^7$ complexes are ferrous nitrosyls with $NO^\bullet$ character, a bent Fe–N–O angle and $\upsilon_{NO} \approx 1670\,cm^{-1}$, as observed for several crystal structures of the corresponding Fe metalloporphyrin nitrosyl complexes [111]. Besides the above-mentioned complexes, iron porphyrins can yield also $\{FeNO\}^8$ complexes, which are supposed to have NO^- (nitroxyl) character, as will be described later [112]. Concerning their stability, the $\{FeNO\}^7$ complexes are by far the most stable ones, with $K_d \approx 10^{-14}$ due to fast NO association to Fe(II) porphyrins (ca. $10^9\,M^{-1}\,s^{-1}$) and very slow NO dissociation [113]. On the other hand $\{FeNO\}^6$ species show lower association rates (ca. $10^6\,M^{-1}\,s^{-1}$), and significantly higher NO dissociation rates (between 1 and $500\,s^{-1}$) [113]. A final very important point concerning the $\{FeNO\}^6$ complexes is their reactivity towards nucleophiles, usually OH^- and nitrite, which results in the reduction of the porphyrin metal center and the oxidation of $NO^\bullet$ to NO_2^- in a process called reductive nitrosylation. The net outcome of the reductive nitrosylation reaction is the formation of $\{FeNO\}^7$ species, when excess NO reacts with ferric porphyrins [114,115]. For a recent review of the above-described reactions, see the review by Ford and coworkers [104].

Manganese porphyrins also form nitrosyl complexes. Fast (ca. $10^6\,M^{-1}\,s^{-1}$) reaction of Mn(II) with $NO^\bullet$ yields stable $\{MnNO\}^6$ complexes [116], that show a linear Mn–N–O geometry [117]. Interestingly, no reductive nitrosylation is observed for Mn(III) reaction with NO [116]. Cobalt porphyrins also form stable nitrosyl complexes. The $\{CoNO\}^8$ species obtained for example by reaction of NO with Co(II) porphyrins have been explored as isoelectronic models for oxygenated heme [118]. The $\{CoNO\}^8$ complexes are very stable, with high association and low NO dissociation rates (with values of ca. $10^9\,M^{-1}\,s^{-1}$ and ca. $10^{-4}\,s^{-1}$, respectively) [113,119]. On the other hand, the $\{CoNO\}^7$ complexes are less stable, with significantly lower association rates [119].

A final interesting point in relation to iron nitrosyl complexes directly related to HNO/NO^- chemistry concerns the nitric oxide reductase (NOR) reaction mechanism, as recently reviewed by Karlin [120]. The NOR reaction is proposed to occur by the binding of two NO molecules to two closely positioned ferrous hemes, which leads to N—N coupling and $N_2O_2^{2-}$ formation (i.e. NO^- dimerization), which finally leads to N_2O, H_2O and two ferric hemes [121,122]. Collman and coworkers succeeded in the synthesis of an inorganic functional model of NOR, containing an iron porphyrin center and a non-heme iron tri/tetra coordinated to imidazole and/or pyridine ligands, which reacts with two equivalents of NO to yield N_2O in the fully reduced state [123,124]. Analysis of possible intermediates by EPR, Resonance Raman and IR spectroscopy lead to suggest the existence of two different nitrosyl intermediates, assigned to mono and dinitrosyl species [123]. The NOR reaction, as described, can therefore be interpreted as a coordination-mediated HNO/NO^- dimerization, depending on the order of ligand reduction, protonation and N—N bond formation steps.

In summary, several metalloporphyrin nitrosyl complexes have been obtained, and kinetically characterized. In the case of Fe, Mn, and Co as metal centers, the same nitrosyl complexes can be obtained by reaction of the corresponding M(III) porphyrins with HNO as will be described in the following sections.

2.2. Reactions of HNO with Fe porphyrins

The first studied reactions of azanone with Fe porphyrins, were not with isolated porphyrins, but directly with myoglobin, the benchmark of the heme proteins. Studies by Farmer and coworkers showed in 2004 that HNO can bind to ferrous deoxymyoglobin forming a stable Fe(II)(Mb)HNO adduct [125]. More recent studies also showed that the Fe(II)(Gb)HNO complex can be obtained with globins such as hemoglobin, leghemoglobin and the SH_2 binding globin from the clam *L. pectinata* [95,126]. Although the difference in the Soret and Q visible bands between the Fe(II)(Prot)NO and the corresponding Fe(II)(Prot)HNO complexes are relatively small, the last complexes are clearly identified by the characteristic peaks at

ca. 15 ppm in the ^{1}H NMR spectra. Further evidence for the formation of Fe(II)(Prot)HNO is obtained by generating the corresponding H^{15}NO adducts, which produce splitting of the HNO resonance in the ^{1}H NMR spectra, since ^{15}N is an NMR-active nucleous with $s = 1/2$. Surprisingly enough, until 2003 no study had been done for the reaction of ferric porphyrins with HNO donors, although preliminary studies with heme proteins had been reported [127].

In this context, the reaction of azanone with isolated iron porphyrins seemed to be a relevant study to be carried out. The first experiments involved the reaction of common, previously described HNO donors such as trioxodinitrate (Angeli's Salt, AS) and toluensulfohydroxamic acid (a Piloty's acid derivative, TSHA), with several model porphyrins, including the water soluble anionic meso-tetrakis(4-sulfonatophenyl) porphyrinate [Fe(III)TPPS]$^{3-}$, the cationic meso-tetrakis-N-ethyl pyridinium-2yl porphyne [Fe(III)TEPyP]$^{5+}$, as well as the pentacoordinated heme-protein model microperoxidase-11 (Fe(III)MP11) and the neutral meso-tetraphenyl porphyrinate (Fe(III)TPP) which is soluble in organic media [128–130].

As expected, all porphyrins yielded the corresponding {FeNO}^{7} complexes, according to the general reaction 29.

$$^1\text{HNO} + \text{Fe(III)Por} \rightarrow \text{Fe(II)PorNO} + \text{H}^+ \quad (29)$$

The reactions can be followed spectroscopically based on the corresponding reported spectral changes characteristic of the starting ferric and nitrosyl porphyrins, respectively. The observed changes in the position of the Soret and Q bands are however moderate.

Although ferrous heme proteins form stable Fe(II)(Prot)HNO adducts, as described above, isolated porphyrins such as FeTPPS or FeTPP do not, clearly suggesting that without the protection provided by the protein matrix the Fe(II)(Prot)HNO (or NO$^-$) adducts are unstable. We will describe below the obtention of the first stable {Fe(Por)NO}^{8} porphyrin model, thanks to the presence of strongly electron-withdrawing substituents present in the porphyrin ring.

2.3. Stabilization of {M(Por)HNO}^{8} complexes by Fe and Ru porphyrins

The first evidences of the existence of {Fe(Por)HNO}^{8} porphyrinate complexes were obtained from the pioneering spectroelectrochemical experiments with Fe(TPP)NO and Fe(OEP)NO carried out by Kadish and coworkers [131,132]. Although cyclic voltammetry showed a well-defined, reversible one electron reduction of Fe(Por)NO, bulk electrolysis in CH_2C1_2 or pyridine did not allow the isolation of [Fe(Por)NO]$^-$, even after the addition of more than 10 equiv of electrons, and the electronic spectra showed only the starting material Fe(Por)NO. From the analysis of the current–time curves it was proposed that a catalytic reaction in which Fe(Por)NO$^-$ reacted with solvent, supporting electrolyte, or possibly trace amounts of oxygen was the reason for the instability of the reduced product. However, cyclic voltammetry experiments with an OTTLE cell showed reversible one-electron transfers that allowed UV–vis characterization of the reduced [Fe(Por)NO]$^-$ products. Since there were minor changes in the Soret bands after reduction, it was concluded that the porphyrin ring was not the site of electron-transfer.

Almost ten years later, Ryan et al. prepared [Fe(TPP)NO]$^-$ in THF solution by both electrochemical and chemical reduction, and afforded further structural and reactivity insight [133]. While the dichloromethane solutions of [Fe(TPP)NO]$^-$ gave back the {FeNO}^{7} precursor within one hour even at low temperatures, the product was indefinitely stable in carefully deoxygenated and dried THF, which allowed Raman spectroscopic characterization. The porphyrin bands were consistent with an Fe(II) diamagnetic product. The ν_{NO} decreased 151 cm^{-1} while the $\nu_{Fe\text{-}N(O)}$ increased 24 cm^{-1} after reduction, consistent with the addition of the electron to the half-filled iron d_z^2 + NO π^* orbital. More recently, FTIR spectroelectrochemical measurements and computational studies were done for [Fe(OEP)(NO)], confirming that the first reduction is highly centered on the FeNO moiety [134]. The reaction of [Fe(TPP)NO]$^-$ with weak acids was also studied; the protonated product, the putative HNO complex, was not stable and oxidized back to the {FeNO}^{7} complex, as judged by UV–vis spectra. The addition of 2-chlorophenol to a solution of Fe(TPP)(NO)$^-$ generated 1 equivalent of hydrogen, as determined by gas chromatographic headspace analysis, Eqs. (30) and (31).

$$[\text{Fe(TPP)NO}]^- + \text{2-ClC}_6\text{H}_4\text{OH} \rightarrow \text{Fe(TPP)HNO} + \text{2-ClC}_6\text{H}_4\text{O}^- \quad (30)$$

$$\text{Fe(TPP)HNO} \rightarrow \text{Fe(TPP)NO} + (\tfrac{1}{2})\text{H}_2 \quad (31)$$

Similar reactivity studies were carried out in aqueous solutions using the water-soluble iron porphyrin Fe(TPPS) [135–137]. The electrocatalytic reduction of nitrite in the presence of the Fe(III) porphyrin in acid solutions yielded ammonia, N_2O and small amounts of N_2. The formation of N_2O was attributed to the protonation and dimerization of [Fe(TPPS)NO]$^-$, obtained from reduction of Fe(TPPS)NO at a potential of −0.65 vs. SCE. Additional studies with the less electron-rich porphyrin Fe(TMPyP) showed a very similar reactivity.

Although, as mentioned above, isolated iron porphyrins seemed unable to present stable {Fe(Por)HNO}^{8} complexes, a fairly stable {Ru(Por)HNO}^{8} complex, [Ru(TTP)(HNO)(1-MeIm)], was obtained, without the support of a protein environment, suggesting additional source of stabilizations of the HNO-porphyrin moiety [138]. Remarkably, this complex is the only Ru(Por)HNO adduct reported, although there are a variety of non-porphyrinic HNO complexes with Re, Os, Ir, Ru and Fe metals [139,140]. The {Ru(Por)HNO}^{8} complex was obtained by hydride attack of the {Ru(Por)NO}^{6} precursor and was characterized by IR and ^{1}H NMR spectroscopies. The HNO signal in the ^{1}H NMR spectrum and the ν_{NO} matched well with the values obtained for (Mb)HNO described previously [196,197].

Apparently, the main reason for the elusive nature of the {Fe(Por)HNO}^{8} complexes previously reported is the high ease of oxidation to the stable {Fe(Por)NO}^{7} form. However, in a recent work, authors were able to synthesize an Fe^{III}(TFPPBr$_8$)Cl porphyrin complex (TFPPBr$_8$ = 2, 3, 7, 8, 12, 13, 17, 18-octa-β-bromo-5, 10, 15, 20-tetrakis-(penta-fluorophenyl) porphyrin), the corresponding {Fe(Por)NO}^{7} nitrosyl iron complex Fe^{II}(TFPPBr$_8$)NO, and strikingly, also its one-electron reduction species, a fairly stable {Fe(Por)NO}^{8} complex which could be isolated as a solid and kept indefinitely under inert atmosphere [112]. The {Fe(Por)NO}^{8} complex, [Co(C$_5$H$_5$)$_2$]$^+$ [Fe(TFPPBr$_8$)NO]$^-$, was obtained from reduction of Fe^{II}(TFPPBr$_8$)NO with the one-electron reductant cobaltocene, and according to FTIR, UV–vis, ^{15}N NMR and DFT results, its electronic structure was assigned as intermediate between Fe^{II}(Por)NO$^-$ and Fe^{I}(Por)NO, which is in sharp contrast with the predominant Fe^{II}(Por)NO$^-$ character of known *non-heme* {Fe(Por)NO}^{8} complexes [94,141]. The enhanced stability with respect to [Fe(TPP)NO]$^-$ and [Fe(OEP)NO]$^-$, the only previously reported nitroxyl-iron porphyrin complexes, was achieved due to the electron withdrawing groups present in the porphyrin ring. Moreover, since there is a second, well reversible reduction wave in the cyclic voltammogram of Fe^{II}(TFPPBr$_8$)NO, its second reduction product, [Fe(NO)(TFPPBr$_8$)]$^{2-}$, was also characterized [142]. The product is stable enough in solution so that the FTIR and UV–vis spectra could be measured. Although, in principle, the formation of an NO^{2-} ligand could be expected, the N–O stretching IR band shifted to higher frequencies (instead of lower). DFT calculations predict this observed shift to higher frequencies only for the intermediate- and high-spin states of [Fe(NO)(TFPPBr$_8$)]$^{2-}$.

Interestingly, while the perhalogenated porphyrin resulted an appropriate platform to stabilize the Fe(Por)NO$^-$ moiety, attempts to protonate [Fe(TFPPBr$_8$)NO]$^-$ to give the expected Fe(Por)HNO complex were unsuccessful, obtaining back the {Fe(Por)NO}^{7} precursor, as previously reported for [Fe(TPP)NO]$^-$. UV–vis and FTIR spectra of the reaction of [Fe(NO)(TFPPBr$_8$)]$^-$ with one equivalent of triflic acid indicate that there is back-oxidation to Fe(NO)(TFPPBr$_8$), probably with the intermediacy of a Fe^{II}(HNO) complex and the formation of H_2, as shown in Eq. (34). However, no reaction is observed when one equivalent of acetic acid is added to [Fe(NO)(TFPPBr$_8$)]$^-$, which indicate that this complex is much less basic than [Fe(TPP)NO]$^-$, as expected for the inductive effect of the withdrawing substituents.

$$[Fe(TFPPBr_8)NO]^- + CF_3SO_3H \rightarrow Fe(TFPPBr_8)NO + (1/2)H_2 + CF_3SO_3^- \quad (32)$$

The difference in stabilities of the six-coordinate complexes (Mb)HNO and Ru(TTP)HNO(1-MeIm) compared to the five-coordinate protonated [Fe(TFPPBr$_8$)NO]$^-$ may be attributed to extra stabilization by distal aminoacids or the ruthenium metal center, though the *trans* ligand may also have an important role in the enhanced stability.

The first reported pK_a value of free HNO in 1970 was 4.7 [143], but new experiments developed in 2002 showed that the correct value for the singlet species ^{1}HNO is likely to be close to 11.5 [79,89]. For the metal HNO-adducts reported so far in aqueous solution, namely Fe^{II}(Gb)HNO and [Fe^{II}(CN)$_5$HNO]$^{3-}$, the pK_a of coordinated HNO could be determined only for the pentacyanoferrate complex. Analysis of the HNO ^{1}H NMR signal at 20 ppm during pH titration indicated a pK_a value of 7.7, lower than the value for free HNO, as expected due to coordination to a cationic metal center [94]. On the other hand, for Fe(II)(Mb)HNO, a change in the ^{1}H NMR signal due to HNO at 14.8 ppm was not observed from pH 6.5 to 10, suggesting a pK_a higher than 10 [125]. Unfortunately, a ^{1}H NMR titration experiment could not be accomplished in this case since protein samples at higher pH are unstable over time and thus unsuitable for NMR studies. However, a rough estimation of the pK_a value could be obtained from the observed changes in the electronic absorption spectra at different pHs. The high-energy band of Fe(II)(Mb)HNO blue shifts at pHs above 11, whereas no changes were observed in the spectra of Fe(II)(Mb)NO or Fe^{II}Mb under similar conditions, which suggests that the pK_a of the HNO adduct is above 10, and likely close to 11 [95].

One of the most striking differences in the ^{1}H NMR of Fe(II)(Mb)HNO between pHs 7 and 10 is loss of the signal assigned to the N-H protons on the distal His64, at 8.11 ppm. In addition, the H/D exchange rate of the HNO signal is slow at physiological pH ($t_{1/2} \sim 5.5$ h at pH 8) but increases significantly at higher pHs ($t_{1/2} \sim 16$ or 9 min at pH 9 or 10, respectively). This behavior was attributed to the loss of hydrogen-bonding interactions between the proton of His64 and the oxygen atom of the HNO adduct at high pH. The His64 hydrogen-bonding interaction increases the back-bonding from Fe(II) to the HNO ligand, thus weakening the N—O bond and strengthening the N—H bond. When this interaction is lost at high pH a lowering of the pK_a of coordinated HNO and thus an increase in H/D exchange would be expected [95]. As has been noted, the protein environment in Fe(II)(Mb)HNO has a big influence on the reactivity of this surprisingly stable adduct and the acid–base equilibria is not an exception.

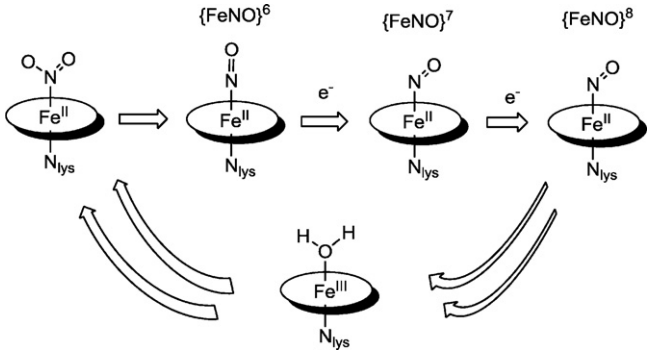

Scheme 3. Reduction of nitrite to ammonia by ccNiR. Proposed mechanism for the formation of the {FeNO}^{8} intermediate [145].

2.4. Characterization of {Fe(Por)HNO}^{8} complexes by electronic structure methods

Computational tools have been employed to check and propose plausible HNO-related species and mechanisms. For example, in cytochrome c nitrite reductase (ccNiR), which catalyzes the reduction of nitrite to ammonia, the active site comprises a protoporphyrin IX covalently linked to the protein backbone, and where the proximal ligand is a lysine [144]. An HNO bound species was proposed as an intermediate in the catalytic cycle. DFT calculations in a simplified model system were used in order to study the reaction pathway [145]. The model comprised an iron porphyrin with proximal ammonia and different reaction intermediates as distal ligands. The choice of the distal ligands was based on crystallographic information. The proposed mechanism (Scheme 3), which is a six-electron reduction, involves as a first step the reduction from Fe(III)–H_2O to Fe(II)–H_2O followed by ligand displacement of water by nitrite in the active site. Next proposed step is heterolytic cleavage of one of the nitrite N—O bonds to produce an {FeNO}^{6} species, which could suffer three likely reactions: protonation of the bound NO$^+$, reduction to {Fe(Por)NO}^{7}, or coupled proton–electron transfer to yield a bound HNO. By calculating the energy cost for each one of this possibilities, the authors suggested that the most attractive mechanism is reduction to {Fe(Por)NO}^{7} followed by a rapid one-electron reduction to {Fe(Por)NO}^{8}. This species can then be protonated to give the HNO bound species. The mechanism continues via a two protons—two electrons step yielding an *N*-bound Fe(II)-hydroxylamine species. The next step involves incorporation of two protons and a reduction via one electron to produce an ammonia bound to an Fe(III) center, which is finally reduced to Fe(II). This species is ready to rebind a new nitrite, displacing the ammonia.

Another interesting case is the mechanism proposed by Lehnert et al. [146]. Using computational tools, the authors have studied the key intermediates in the catalytic cycle of fungal nitric oxide reductase (P450nor). This enzyme converts NO to N_2O via a {FeNO}^{8} species [147–149]. The proposed mechanism (Scheme 4), involves coordination of NO to the Fe(III) form, a reducing step via NADH to yield an intermediate I (an Fe(II)(Por)NOH species) and finally a second reaction with NO to generate N_2O and the Fe(III) form. Intermediate I has been characterized via UV–vis and resonance Raman spectroscopy [150,151].

To get further insight in the biochemistry, the authors modeled the active site of these types of proteins with a six-coordinated model: an iron-porphine, the nitrogenated species (NO, HNO, NOH, $N_2O_2^{2-}$, $N_2O_2H^-$, $N_2O_2H_2$) and 1-methylimidazole or methylthiolate as the proximal ligands. DFT calculations were carried out to fully optimize the structures and to obtain vibrational information. An approximate pK_a for the protonation steps was also calculated

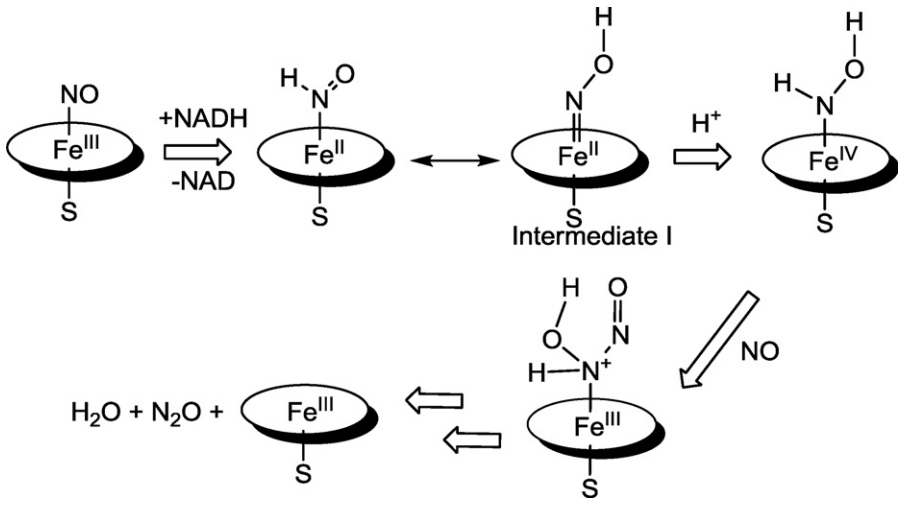

Scheme 4. Proposed mechanism for the conversion of NO into N_2O by P450nor [136–138].

taking into account the solvation effects using an implicit solvent scheme (PCM model). The most interesting feature proposed by the authors is that in contrast with the (Mb)HNO structure reported by Farmer, they suggested that the intermediate comprises a doubly protonated species. This Fe(IV) (Por)NHOH complex can react easily with the second NO molecule. The thiolate role is to stabilize this species and allows the double protonation.

The details of the heme-thiolate nitric oxide reductase (P450nor) catalytic mechanism are still controversial. One theory, supported by computational results [152], assumes two sequential one-electron transfers from NAD(P)H to an initial $\{Fe(Por)NO\}^6$ complex. The $\{Fe(Por)NO\}^8$ species thus formed would react with NO, eventually releasing the $ONNO^{2-}$ anion (most probably in its protonated form), which decomposes to N_2O and water. However, more recent experimental results [153] suggest the first step of the mechanism (Scheme 4) to be direct hydride transfer from NAD(P)H to $\{Fe(Por)NO\}^6$, presumably resulting in an iron-bound HNO unit. DFT geometry optimization of all the proposed reaction intermediates was reported, suggesting that the hydride transfer to $\{Fe(Por)NO\}^6$ could produce $\{Fe(Por)NOH\}^8$ or $\{Fe(Por)HNO\}^8$. Subsequent addition of NO to $\{Fe(Por)NOH\}^8$ (but not to $\{Fe(Por)HNO\}^8$ or $\{Fe(Por)N(H)OH\}^8$ is predicted to lead to immediate liberation of $HN_2O_2^-$, without any stable intermediates, which finally decomposes to H_2O and N_2O. Contrary to what would be predicted according to the "thiolate push effect" dogma, the thiolate ligand at the heme active site obstructs NO reduction, rather than facilitate it. It is in fact shown that replacement of the thiolate by a neutral nitrogen ligand (i.e., lysine, as found in the active site of cytochrome c nitrite reductase, mentioned above) clearly favors, from a thermodynamic point of view, NO reduction at the heme site [154].

Regarding the structural characterization of (Mb)HNO, Linder and Rodgers used DFT calculations on a model system to study the potentials implicants of the different protonation schemes [155]. The calculations were performed for a [Fe(Por)HNO(ImH)] as a heme model for (Mb)HNO. One of the key questions that the authors tried to solve was where was the proton located by calculating several different coordination (O or N) and protonation (HNO or NOH) isomers. The most stable isomer at the used level of theory corresponded to the N coordinated and protonated one. The geometrical parameters are almost insensitive to the rotation of the imidazole ring, suggesting a decoupling of the Fe-N(H)O and Fe-ImH π bonding. Moreover, in the EXAFS structure the imidazole ring remains almost in an eclipsed conformation respect to the pyrrolic ^{15}N atoms [155]. The calculation of this rotated conformation, is only 3.4 kJ/mol higher than the ground state structure. The barrier of rotation around the Fe—N bond is low, suggesting that the ligand conformation can be easily stabilized in the protein due to influences of the environment. Another interesting issue regarding the EXAFS structure of (Mb)HNO was the particular observation of the long Fe—N(HNO) bond despite the high experimental IR frequency for Fe—N. The authors identified a normal mode with a high Fe—N character, which agrees with the experimental shift observation upon N isotopic labeling. The rationalization of the long bond and high IR frequency was attributed to a low effective mass.

Recently, Zhang and coworkers focused on the importance of the computational tools to study compounds involving HNO and porphyrins [156]. Using a quantitative structure observable relationship, the authors performed a large number of quantum calculations on heme models in order to evaluate potential methodologies to predict geometrical parameters: ^1H NMR displacements, ^{15}N NMR displacements and ν_{NO} stretching frequencies of HNO and RNO bound moieties. In particular, the exploration involved Fe and Ru porphyrins with methylimidazole and pyridine as axial ligands and also some non-heme models. Several DFT functional and basis sets were employed, selecting different combinations for each one of the observables proposed. The best method to predict geometrical parameters was a pure DFT functional (mPWVWN). Among the most interesting results, the authors explored the potential effect of water interaction with the HNO bound to an Fe(II) porphyrin, as a model for (Mb)HNO. The calculations suggest that the IR frequency of the bound HNO in myoglobin can be explained by dual H_2O—HNO hydrogen bonding.

2.5. Reactivity of HNO towards Mn and Co porphyrins

Besides the reactivity of azanone with iron porphyrins, other metalloporphyrins, namely with Co or Mn as the metal center, also react with HNO giving raise to interesting applications. When aqueous solutions of AS (at pH 7) or TSHA (at pH 10) are added to $[Mn(III)TEPyP]^{5+}$ under inert atmosphere, in equimolar or slight donor excess ratios, total conversion of $[Mn(III)TEPyP]^{5+}$ to $[Mn(III)TEPyP\text{-}NO]^{4+}$ is observed. Interestingly, and in opposition to what is observed for the Fe^{3+} Porphyrins, there is a significant blue shift (more than 30 nm) of the Soret band, potentially providing a sensitive tool for HNO detection and quantification, as will be discussed in the next section. Similar spectral changes are observed for HNO donor reactions with $[Mn(III)TPPS]^{3-}$, although in these case excess donor is needed for the reaction to be completed, due to kinetic reasons that will be explained below.

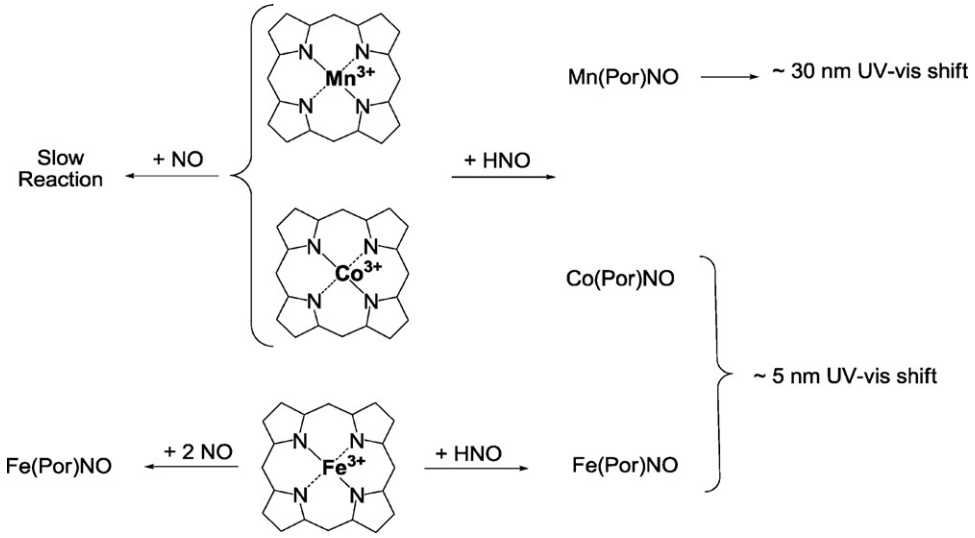

Scheme 5. HNO versus NO reactivities of Mn, Co and Fe porphyrins and UV–vis shifts of the Soret bands for the corresponding M(Por)NO products [128,129,157,158].

However, neither [Mn(III)TEPyP]$^{5+}$ nor [Mn(III)TPPS]$^{3-}$ react with NO(g) or NO donors (such as SNAP) under similar conditions, which means on one hand that the equilibrium constant for the formation of the Mn(III) nitrosyl product is not favorable, and on the other hand that these Mn(III) porphyrins do not suffer reductive nitrosylation to produce the Mn(II)(Por)NO complex as easily as the corresponding Fe(III) porphyrins do. Therefore, Mn(III) porphyrins show selective reactivity towards HNO, while Mn(II) porphyrins are selective for NO (Eqs. 33–36) [128,129].

$$NO + Fe(III)Por \rightarrow Fe(II)(Por)NO \quad (33)$$

$$HNO + Fe(III)Por \rightarrow Fe(II)(Por)NO + H^{+} \quad (34)$$

$$NO + Mn(III)Por \rightarrow Slowreaction/N.R. \quad (35)$$

$$HNO + Mn(III)Por \rightarrow Mn(II)(Por)NO + H^{+} \quad (36)$$

Regarding Co porphyrins, the reaction with HNO of cobalt 5,10,15,20-tetrakis[3-(p-acetylthio-propoxy)phenyl]-porphyrin [Co(P)], which is soluble in organic media, was studied [157]. This porphyrin has four sulfur anchors that allow it to be attached to electrodes, as will be shown later. The reaction of NO(g) with Co^{II}(P) produces Co(III)(Por)NO^{-} in a few minutes, in agreement with previous data for other cobalt porphyrins [158]. In a similar timescale, no spectral changes are observed for Co(II)Por in the presence of the nitroxyl donor TSHA. On the other hand, adding to Co(III)Por TSHA and 1,8-diazabicyclo(5.4.0)undec-7-ene—that accelerates TSHA decomposition in organic solvent by deprotonation-, slowly produces Co(III)(Por)NO^{-}, as confirmed by UV–vis and IR spectroscopy (ν_{NO} = 1679 cm^{-1}). The UV–vis spectral changes are quite small, similarly to what happens with the corresponding reactions of iron porphyrins. In a similar timescale, no reaction takes place for Co(III)Por in the presence of NO(g) or any studied NO donor. The results, similarly to what is observed for Mn porphyrins, clearly show that Co^{II}Por reacts with NO, and not with HNO, while Co^{III}Por reacts with HNO and not with NO [157].

In summary, while iron porphyrins cannot discriminate NO from HNO due to the reductive nitrosylation reaction, both Mn and Co porphyrins tend to differentiate NO from HNO: Co(II) and Mn(II) porphyrins react rapidly with NO but not with HNO, while Co(III) and Mn(III) porphyrins react rapidly with HNO but not with NO. On the other hand, Mn porphyrins tend to show an important shift in the UV–vis spectra (Soret band) when going from Mn(III) to Mn(II)NO porphyrins, while Co and Fe porphyrins do not (see Scheme 5).

2.6. Comparison of the reactivity of HNO and NO towards metalloporphyrins

A key determinant of the fate of nitroxyl in any given media, either *in vivo* or *in vitro*, will depend upon all the competing reaction rates. To study the ^{1}HNO-to-metalloporphyrin association kinetics, the UV–vis spectral changes corresponding to the formation of a nitrosyl porphyrin can be followed as a function of time for each reaction conditions, such as: different donors (SA or TSHA), pH, and relative porphyrin to donor concentration ratios. Plots of the corresponding traces allow the determination of the initial observed rate υ_{obs} for the nitrosylation reaction. Even for reactions performed in strictly anaerobic media to avoid ^{1}HNO/^{3}NO^{-} reactions with O_2, trace amounts of oxygen can be present since it is extremely difficult to remove O_2 from water below 10^{-7} M. The obtained exponential traces of nitrosyl product formation (when extreme ca. 100 donor to porphyrin ratios are used) are strongly indicative that for all cases the reaction is first order in porphyrin. Strikingly, two significantly different reaction times and stoichiometries are observed for peripherical negatively or positively charged iron and/or manganese porphyrins. For negatively charged porphyrins such as [Fe(III)TPPS]$^{3-}$ and [Mn(III)TPPS]$^{3-}$ the reaction with AS at pH 7 (where AS spontaneous decomposition has a half-life of about 900 s) [127,159], requires a large excess of AS to drive the reaction to completion and for an equimolar ratio the reaction half-life is ca. 120 min. On the other hand, the reaction of positively charged porphyrins such as [Fe(III)TEPyP]^{5} and [Mn(III)TEPyP]^{5} total conversion to the nitrosyl metalloporphyrin is obtained with an equimolar porphyrin to donor ratio in less than 10 s. A similar behavior is observed for the reactions with the HNO donor TSHA. These results clearly point to different reaction mechanisms operating depending on the porphyrin peripheral charge. The fact that the overall reaction rate for positively charged porphyrins by far exceeds the donor spontaneous decomposition strongly suggests that a direct porphyrin-donor interaction is taking place and that these porphyrins accelerate their decomposition. Therefore, Scheme 6 was proposed for the reactions of HNO donors with metalloporphyrins.

In Scheme 6, k_{on}(Donor) represents the bimolecular association rate constant of the metalloporphyrin with the HNO donor, k_{cat}(Donor) represents the porphyrin-accelerated donor decomposition rate constant, k_d represents the spontaneous donor decomposition rate constant to yield HNO, and k_{on}(HNO) is the bimolecular metalloporphyrin-to-HNO association rate. In order

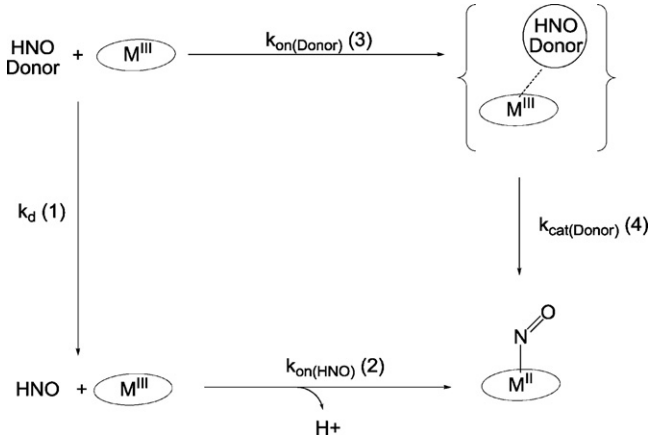

Scheme 6. Proposed mechanism for the reactions of HNO donors with metalloporphyrins [129].

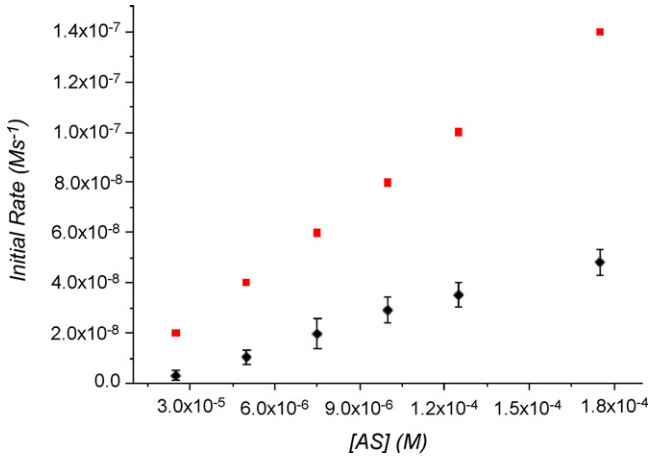

Fig. 2. Nitrosyl product formation rate (diamonds) and estimated HNO production rate (squares) as a function of AS concentration for the reaction of $[Mn(III)TPPS]^{3-}$ with HNO.

to obtain the rate constants the following limiting cases have been analyzed: case (i) for negatively charged metalloporphyrins, the rate of ^{1}HNO production due to spontaneous decomposition (k_{donor}) exceeds the reaction rate of HNO with the metalloporphyrin (k_{on}(HNO)), and the dimerization of HNO competes with the nitrosyl product formation. This is clearly shown in Fig. 2, where the observed nitrosyl product formation rate (diamonds) and the HNO production rate (squares) are plotted against donor concentration. The shape of the υ_{obs} against AS plot is not linear, since when the HNO production is increased (due to an increase in donor concentration) the dimerization rate increases with the square of [HNO], as described by equation 37, and therefore the relation between [HNO] and [Donor] is not linear. However, using the steady state approximation for [HNO] (i.e. assuming that all HNO produced by the donor either reacts with the porphyrin or dimerizes—k_{dim} = dimerization rate constant), the HNO concentration can be estimated according to equation 39. Using the estimated HNO concentration, a plot of υ_{obs} against [HNO] yields as expected a linear plot, which allows determining the bimolecular HNO association rate constant k_{on}(HNO).

$$[HNO] = \left[\frac{(k_{cat(Donor)}[Donor] - \upsilon_{obs})}{k_{dim}}\right]^{1/2} \quad (37)$$

On the other hand, (case ii)) if the reaction of the donor with the metalloporphyrin is faster than its spontaneous decomposition rate, the metalloporphyrin reacts directly with the donor, accelerating its decomposition rate and forming the corresponding nitrosyl complex by azanone transfer to the metal center. For these cases, almost no free HNO is produced, as evidenced by the quantitative formation of the nitrosyl product even for equimolar metalloporphyrin to donor ratios. In these cases, the υ_{obs} against [Donor] plot gives a straight line from which the bimolecular $k_{cat(Donor)}$ rate constant can be obtained.

Further evidence for direct azanone transfer from AS to the metal center was obtained by the kinetic analysis of the reaction at pH 10, where AS is stable. Even under these conditions, the reaction with positively charged Mn porphyrins produces the nitrosyl product stoichiometrically in less than 5 s, while adding AS to the negatively charged $[Mn(III)TPPS]^{3-}$ at pH 10 does not produce any reaction at all. Finally, DFT studies on the direct interaction of AS with both Mn and Fe porphyrins showed that AS ($N_2O_3^{2-}$, $(ON_a{=}N_bO_2)^{2-}$) is able to coordinate to either Mn(III) or Fe(III) by the N_a nitrogen, which results in a significant weakening of the N_a—N_b bond, therefore partially explaining the observed rate acceleration. It is expected that, being negatively charged, AS coordination to the metal center will be faster for positively charged metalloporphyrins.

Using the kinetic analysis described above, k_{on}(HNO) and/or k_{on}(Donor) were obtained for several Mn and Fe porphyrins, and are shown in Table 3.

The data shown in Table 3 is consistent with two alternative pathways for the reactivity of nitroxyl donors (AS, TSHA) in aqueous solutions: HNO transfer to the metal center through reaction of the porphyrin with azanone or with the HNO donor (see Scheme 6 above). Interestingly, and despite the fact that k_{on} for HNO binding are faster than k_{on} for the donors, donor concentrations are usually four orders of magnitude higher than those of HNO. Therefore, depending on the donor and porphyrin concentrations, one or the other pathway will predominate. At relatively high concentrations (10^{-4}, assuming a 1:1 = donor:porphyrin ratio) a faster rate is observed for the direct reaction with the donor, as initially observed for Mn(III) cationic porphyrins [129] and later also for the ferric analogues [130].

Concerning the direct reaction between the donor and the metalloporphyrin, a redox mechanism could be operative for TSHA. Piloty's acid are oxidized by several iron complexes yielding the corresponding radical, which decomposes to produce NO and the reduced metal complex [160]. This mechanism would imply that the reaction proceeds through an intermediate state with the reduced porphyrin (Fe(II)), TSHA radical and free NO. Afterwards, NO would react very fast with the reduced iron porphyrin yielding the corresponding nitrosyl complex as the final product, as observed here. However, a mechanism involving an intermediate formed by TSHA and the metalloporphyrin followed by NO^- transfer to the porphyrins cannot be discarded and both mechanisms are compatible with the experimental observations. More interestingly, recent obtained data for a negatively charged bromated porphyrin $[MnBr_8TPPS]^{3-}$, indicates that the actual followed reaction mechanism (reaction of the porphyrin with nitroxyl or with the HNO donor) depends more likely on the reduction potential of the porphyrin metal center, than on its peripheral charge. This is evidenced from the data in Table 3 showing that the negatively charged $[MnBr_8TPPS]^{3-}$, having a positive reduction potential due to the presence of the electron-attracting bromine substituents, reacts directly with the HNO donor, the same as the positively charged $[MnTEPyP]^{5+}$. However, the negatively charged $[MnTPPS]^{3-}$, with a reduction potential of −160 mV, reacts via the free HNO pathway.

The abovementioned scenario becomes even more complex in the presence of dioxygen, due to the reactivity of HNO and the M(Por)NO porphyrins towards O_2. These reactions give place

Table 3
Kinetic rate constants for the reactions of Mn(III) and Fe(III) porphyrins with AS and TSHA.

Porphyrin (III)	$E_{1/2}$ $M^{3+/2+}$ vs NHE*	$k_{on\,(donor)}$ ($M^{-1}\,s^{-1}$)		$k_{on\,(HNO)}$ ($M^{-1}\,s^{-1}$)		Ref.
		AS (pH 7)	TSHA (pH 10)	AS (pH 7)	TSHA (pH 10)	
$[MnTEPyP]^{5+}$	+220 mV	1.2×10^4	1.0×10^4	–	–	[106]
$[MnBr_8TPPS]^{3-}$	+209 mV	3.7×10^3	7.9×10^3	–	–	PC[a]
$[FeTEPyP]^{5+}$	+380 mV	5.4×10^3	1.1×10^4	–	–	[46,130]
$[FeTPPS]^{3-}$	+23 mV	0.5	–	1.0×10^6	–	[97]
$[MnTPPS]^{3-}$	−160 mV	–	–	$\sim 4.0 \times 10^4$	$\sim 9.0 \times 10^4$	[129]
[FeMP11]	−360 mV	–	–	6.4×10^4	3.1×10^4	[46,130]

[a] PC = Doctorovich and coworkers, personal communication.

Table 4
Kinetic rate constants for the relevant reactions of $[Mn(TPPS)]^{3-}$ with AS.

#	Reaction	Value	Ref.
1	$HONNOH \rightarrow N_2O$	$5 \times 10^{-4}\,s^{-1}$	[67]
2	$HNO + HNO \rightarrow HONNOH$	$8 \times 10^6\,M^{-1}\,s^{-1}$	[66]
3	$AS \rightarrow HNO + NO_2^-$	$2.30 \times 10^{-3}\,s^{-1}$	[54,56–59]
4	$[Mn^{3+}(TPPS)]^{3-} + HNO \rightarrow [Mn^{2+}(TPPS)NO]^{3-}$	$1.0 \times 10^5\,M^{-1}\,s^{-1}$	[129]
5	$AS + [Mn^{3+}(TPPS)]^{3-} \rightarrow [Mn^{2+}(TPPS)NO]^{3-} + NO_2^-$	$20\,M^{-1}\,s^{-1}$	PC[a]
6	$O_2 + [Mn^{2+}(TPPS)NO]^{3-} \rightarrow [Mn^{3+}(TPPS)]^{3-} + NO_3^-$	$5\,M^{-1}\,s^{-1}$	PC[a]
7	$O_2 + HNO \rightarrow H^+ + NO_3^-$	$5 \times 10^3\,M^{-1}\,s^{-1}$	([b])

[a] MP = Doctorovich and coworkers, personal communication.
[b] This reaction has to be considered as: (7a) $O_2 + HNO \rightarrow HO_2 + NO$ $k_{7a} = 5 \times 10^3\,M^{-1}\,s^{-1}$ (average of lit. rate constants) [18,26]; (7b) $HO_2 + NO \rightarrow ONOOH$ $k_{7b} = 5 \times 10^9\,M^{-1}\,s^{-1}$ [82]; (7c) $ONOOH \rightarrow H^+ + NO_3^-$ $k_{7c} = 1.2\,s^{-1}$ [161]; As the reactions 2 and 3 are very fast, and the intermediates have been obviated, we decided to use k_{7a} as the value for reaction 7.

to oxygen and nitrogen reactive species (ORS and NRS) such as $ONOO^-$, NO, NO_2, HO_2, and others. The most important effects due to the presence of oxygen are the oxidation of the M(II)(Por)NO product back to the M(III)(Por) starting material [129] and the consumption of HNO, therefore lowering its effective concentration. In order to analyze this scenario a set of more than 20 reactions involving the porphyrins as well as the ORS and NRS have to be taken into consideration (see Appendix A). By using numerical simulations which take into consideration all the rate laws and kinetic constants involved, it can be demonstrated that in order to describe correctly the kinetic reaction profiles at pH 7, only 7 reactions are needed, which are shown in Table 4 and Scheme 7 for $[Mn(TPPS)]^{3-}$ with AS as the HNO donor.

Scheme 7 Reactions involved in the kinetic simulations which describe appropriately the reaction of metalloporphyrins with AS ($HN_2O_3^-$) in the absence and presence of dioxygen, at pH 7 [54,56–59,66,67,129].

Under anaerobic conditions, AS in solution decomposes to produce only nitrite and HNO, which dimerizes yielding nitrous oxide. However, if O_2 is present at a high concentration compared to AS, nitrate and nitrate are the main reaction products and nitrous oxide is practically not formed due to the competing reaction of HNO with O_2 to presumably produce initially HO_2 and ultimately NO_3^- and NO_2^- (only the formation of NO_3^- by this route was considered, see footnote b in Table 4 and dotted lines in Scheme 7). Therefore, when the metalloporphyrin and AS coexist in solution under anaerobic conditions, the reaction of HNO with the M(III)Por competes not only with its dimerization but also with O_2. Moreover, since the M(II)PorNO product also reacts with O_2 to produce the starting material back, little or no product is observed for relative low concentrations of AS and metalloporphyrin compared to O_2. On the contrary, when the concentrations of both AS and metalloporphyrin are at least one order of magnitude higher than $[O_2]$, the M(II)PorNO product is formed and stays in solution.

All the above observations could in principle be applied to other metalloporphyrins and/or HNO donors different from $[Mn(TPPS)]^{3-}$ and AS. The kinetic profiles should heavily depend on the most important rate constants involved, which are k_4 (k_{on}(HNO)), k_5 (k_{on}(donor)) and k_6 (k_{ox}(MPorNO). The rate constant

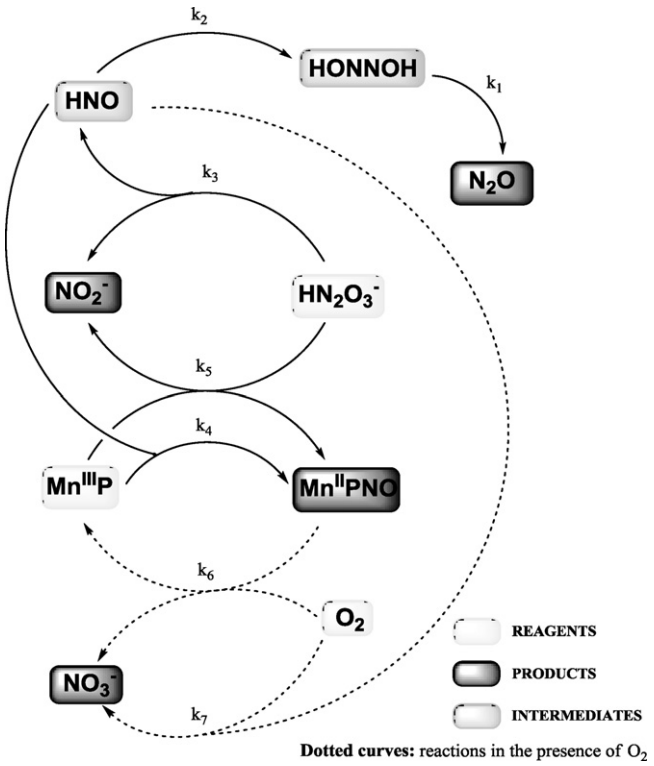

Scheme 7. Reactions involved in the kinetic simulations which describe appropriately the reaction of metalloporphyrins with AS ($HN_2O_3^-$) in the absence and presence of dioxygen, at pH 7 [54,56–59,66,67,129].

k_4 ranges from 10^4 to $10^6\,M^{-1}\,s^{-1}$, k_5 from 1 to $10^4\,M^{-1}\,s^{-1}$ and k_6 still has to be determined for a set of metalloporphyrins, although it can be estimated that for the metalloporphyrins with positive reduction potentials its value should be below $5\,M^{-1}\,s^{-1}$ (Table 4).

Finally, Table 5 shows a comparison of the rate constants for the reactions of HNO and NO with metalloporphyrins and heme proteins. It is clear from the data presented, that although lacking the

Table 5
Bimolecular rate constants for HNO and NO binding to metalloporphyrins and heme proteins.

Target	Reactant	k_{on} (M^{-1} s^{-1})	Ref.
Fe(III)MP11	HNO	$3.1–6.4 \times 10^4$	[130]
Fe(III)MP11	NO	1.1×10^6	[163]
$[Fe(III)TPPS]^{3-}$	NO	4.5×10^5	[113]
metMb(Fe(III))	HNO	8×10^5	[18]
metMb(Fe(III))	NO	4.9×10^4	[18,164,165]
catalase(Fe(III))	HNO	3×10^5	
$[Fe^{II}TPPS]^{4-}$	NO	1.5×10^9	[113]
Mb(Mn(III))	HNO	3.4×10^5	[166]
Mb(Fe(II))	HNO	1.4×10^4	[125]
O_2	HNO	3×10^3	[18]

protein scaffold, the soluble porphyrins and MP11 display reactivity towards HNO comparable to the observed reactivity of HNO with heme proteins [18]. The bimolecular rate constants for HNO binding to ferric heme systems are in the order of 10^5 to 10^6 M^{-1} s^{-1}, similar to the values obtained for NO and probably represent an upper limit for the reaction with ferric hemes. However, these rates are more than 1000 times lower than the corresponding values for NO or CO binding to ferrous hemes [113]. This trend can be explained due to the fact that, for ferric hemes, the ligand binding rate is usually dependent on the lability of the leaving water ligand, in contrast with ferrous hemes, where the water ligand is weakly bound [113]. This fact plays a key role in ligand binding rates in heme proteins [162], therefore it is also expected to be determinant for hem reactivity with HNO.

3. Detection of nitroxyl

3.1. Spectroscopic methods

3.1.1. Colorimetric methods

The high efficiency by which ferric porphyrins trap HNO, and the observed stability of $\{Mn(Por)NO\}^6$ but not $\{Mn(Por)NO\}^5$ complexes, suggested to test Mn(III) porphyrins as agents for HNO/NO discrimination. As mentioned in a previous chapter, differently from Fe(III) porphyrins, Mn(III) porphyrins do not suffer reductive nitrosylation in the timescale of the reaction with HNO, and, the conversion of Mn(III) porphyrins to Mn(II)(Por)NO results in a large shift of the UV–vis Soret band. Moreover, since water-soluble metalloporphyrins (such as Mn(III)TPPS) or others which are soluble in organic solvents (such as Mn(III)TPP) can be used and show a similar shift, the method is useful for organic or aqueous solutions. An important disadvantage for this reaction is that the Mn(II)(Por)NO porphyrin obtained as a product reacts with O_2 to reproduce the starting Mn(III) back. Based on these data, Dobmeier et al. found a way to overcome this inconvenience [167], and designed a method for quantitative detection of nitroxyl with an estimated dynamic range of 24–290 nM. This optical sensor film, suitable for the quantitative determination of HNO, was obtained through encapsulation of Mn(III)TPPS within the anaerobic local environment of an aminoalkoxysilane xerogel membrane decorated with trimethoxysilyl-terminated poly(amidoamine-organosilicon) dendrimers, which are poorly O_2-permeable. This HNO-sensing films were tested with the HNO donors AS and sodium 1-(isopropylamino)diazene-1-ium-1,2-diolate (IPA/NO), and were found to provide a rapid means for determining HNO concentrations in aerobic solution. However, the rapid dimerization of HNO and relatively slow rate of HNO complexation in the xerogel film limit optimal sensor performance to environments with restricted HNO scavenging conditions and renders a narrow dynamic range.

Another way to circumvent the problem raised by the reactivity of the nitrosyl product towards O_2 is to protect the metalloporphyrin by a protein matrix which slows down the oxidation rate. Mn^{III} protoporphyrinate IX recombined into apomyoglobin reacts with AS, while it remains indifferent towards NO or NO donors, either under anaerobic or aerobic conditions [166]. The association rate constant for the reaction of the reconstituted globin with the nitroxyl donor is practically the same than that for the free porphyrinate, suggesting that the protein environment is not involved in the association reaction mechanism. However, in contrast to what happens to the free porphyrinate, the Mn(II)(Por)NO reaction product results to be significantly stable in the presence of oxygen when the porphyrinate is included in the protein matrix; this feature is ascribed to the role of the distal aminoacidic residues on the metal center.

Another colorimetric method uses the reaction of HNO with nitrosobenzene to form the indicator cupferron (*N*-nitrosophenylhydroxylamine) [168]. However, this method is limited to organic solvents.

A main disadvantadge to be taken into account for all these colorimetic methods is that, due to the fact that the UV–vis measurements are done in a wavelength range where biological materials strongly absorb, these optical methods cannot be used for most *in vitro* or *in vivo* studies.

3.1.2. Fluorescent detection

Several proposed methods use non-heme fluorescent probes for HNO detection. Oxidation of dihydrorhodamine by two-electron oxidants produces rhodamine, which is fluorescent and can be detected at 570 nm with excitation at 500 nm. This method has been used for the indirect detection of NO^- by reaction with O_2, being peroxynitrite the proposed intermediate which oxidizes dihydrorhodamine [169].

More recently, Lippard and coworkers developed two compounds for fluorescent detection of nitroxyl. The first one is a bithiophene-substituted poly(p-phenyleneethynylene) derivative (CP1) which forms a Cu(II) complex that becomes fluorescent upon exposure to excess NO in unbuffered solutions, but under simulated biological conditions (pH 7.4 buffer) it shows a small decrease in emission upon treatment with NO, probably as a consequence of precipitation of the probe [170]. A 2-fold increase in CP1–Cu(II) integrated emission occurs upon exposure to AS, indicating that CP1–Cu(II) can sense HNO selectively over NO in buffered aqueous solutions, taking into account its apparent insensitivity to NO.

The second probe, BOT1 (see Fig. 3), comprises a BODIPY reporter site, which has optical properties that are well suited for cellular imaging experiments and a tripodal coordination environment provided by a N-(triazolylmethyl)-N,N-dipicolyl framework, both separated by a triazole bridge as a rigid spacer [171]. This design minimizes the distance between fluorophore and metal binding site, thereby assuring strong fluorescence quenching in the probe off-state. While after excitation at 518 nm BOT1 shows emission at 526 nm and Φfl = 0.12, by coordination to Cu(II) the fluorescence intensity decreases to Φfl = 0.01 and the lifetime by

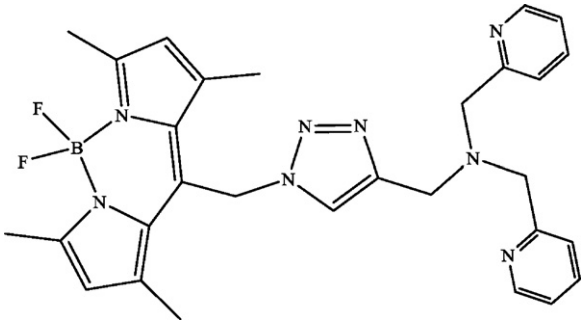

Fig. 3. Structure of BOT1.

30-fold. However, if Cu(II) is reduced to Cu(I) by an excess of cysteine, the emission is restored. When Cu(II)[BOT1] is treated with excess AS in buffered solutions, a ca. 4-fold increase in emission was observed with the concomitant formation of NO(g), and possibly Cu(I)[BOT1]. NO_2^- and other RNS and ROS such as NO, NO_3^-, $ONOO^-$, H_2O_2 and OCl^-, failed to induce significant emission enhancement of the Cu(II)[BOT1] complex. The complex was also tested in HeLa cells: addition of AS to this cells increased the observed intracellular red fluorescence over the course of 10 min, consistent with an HNO-induced emission response.

3.1.3. EPR detection

Xia and coworkers examined the trapping specificity of different redox forms of Fe-MGD (N-methyl-D-glucamine dithiocarbamate iron). According to the authors, with Fe(II)-MGD, NO generates characteristic triplet NO•-Fe(II)-MGD signals, whereas HNO from AS is EPR silent. Both NO and NO^- give rise to NO•-Fe(II)-MGD signals when Fe(III)-MGD is used. The authors asseverate that "spin trapping with Fe-MGD can distinguish NO and NO^- and this depends on the redox status of the iron center" [172]. However, an EPR signal would be observed if only NO is present, as well as if both NO and HNO are coexisting in the solution. Therefore, this method cannot discriminate HNO from NO. In another publication, Komarov and coworkers [173] showed that in the presence of dioxygen Fe(II)-MGD reacts with AS or AS-derived NO^- to yield NO•-Fe(II)-MGD, possibly by reaction of NO^- with Fe(III)-MGD formed by aerobic oxidation of the iron center. Since the paramagnetic NO•-Fe(II)-MGD complex is produced by AS (and/or NO^-), and also by NO, dithiocarbamate iron traps do not distinguish between NO and NO^-.

More recently, the nitronyl nitroxides 2-phenyl-4,4,5,5-tetramethylimidazoline-l-oxyl 3-oxide (PTIO) and its water soluble analogue 2-(4-carboxyphenyl)-4,4,5,5-tetramethylimidazoline-1-oxyl 3-oxide (C-PTIO) have been investigated as NO/HNO discriminating agents [174]. Nitronyl nitroxides are known to react with NO producing the corresponding imino nitroxides, which are detectable by EPR [175]. C-PTIO and PTIO are reduced by HNO and converted into their respective imino nitroxides or imino hydroxylamines, both detectable by EPR. The yield of the imino hydroxylamine increases at the expense of the imino nitroxide – also produced by reaction with NO – with an increase in the ratio $[AS]_0/[\text{nitronyl nitroxide}]_0$, where $[AS]_0$ represents the total production of HNO. Therefore, nitronyl nitroxide can discriminate between NO and HNO only at high $[AS]_0/[\text{nitronyl nitroxide}]_0$ ratios.

3.2. Electrochemical methods

Metalloporphyrins, are widely used in technical applications, including gas sensors [176,177] when coupled to a surface. Ordered monolayers of metalloporphyrins can be easily built, specially when surface molecule linking is based on the establishment of Au—S bonds, and a number or thiol bearing porphyrins are available. Furthermore, the use of S-acetyl protecting groups, that undergo *in situ* cleavage on the surface allows the obtention of single porphyrin layers in a straightforward manner. Based on the previously described cobalt porphyrins reactivity towards NO and HNO (section 2.5), and the common use of surface-modified electrodes as electrochemical sensors, a porphyrin with four anchors, Co(II)-5,10,15,20-tetrakis[3-(p-acetylthiopropoxy) phenyl]porphyrin (Co(Por), shown in Fig. 4), was immobilized on a gold surface by the formation of Au—S bonds [157]. Both XPS and STM techniques show that most Co(Por) molecules are adsorbed in the lying down configuration by multiple linker binding to the gold surface, and that vacant gold sites are present that can be occupied in some cases by smaller lateral size adsorbates.

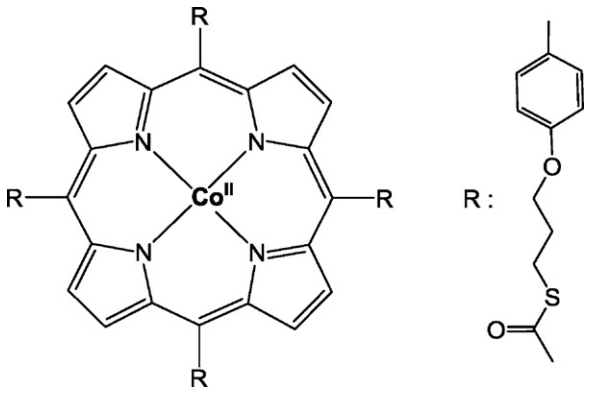

Fig. 4. Co(II)-5,10,15,20-tetrakis[3-(p-acetylthiopropoxy) phenyl]porphyrin.

The reactions of HNO and NO with electrode bound Co(Por), were studied by electrochemical techniques. Previous studies by Kadish and coworkers showed that for nitrosyl complexes of Co(Por) in solution, four redox couples are found corresponding to the equilibria between $[Co(Por)NO]^{+2}$, $[Co(Por)NO]^{+1}$, $Co^{III}(Por)NO^-$, $[Co(Por)NO]^-$ and $[Co(Por)NO]^{2-}$ states [178].

Electrochemical measurements of Co(Por) bound to electrodes show the presence of three redox couples, as well as the electrode bound nitrosyl porphyrin complex. The most significant feature of the electrochemical data is that for Co^{III}/Co^{II} couple (Eq. 37), the obtained $E_{1/2}$ value is shifted ca. 400 mV to lower potentials compared to the $E_{1/2}$ in solution, strongly suggesting that Co(Por) adsorption on the gold electrode facilitates Co^{II} oxidation. On the other hand, for the nitrosyl porphyrin the shift due to the gold surface effect is much smaller than before, and of only 60 mV (Eq. 38). This is ascribed to charge donation from the gold surface which stabilizes the Co(III) state in $[Co(III)(Por)]^+$. This Co—Au interaction is weakened by NO coordination to the metal center.

$$[Co(III)(Por)]^+ + e^- \rightleftharpoons \mathbf{Co(II)(Por)} \quad (37)$$

$$[Co(III)(Por)NO]^+ + e^- \rightleftharpoons [\mathbf{Co(III)(Por)NO^-}] \quad (38)$$

Both NO and HNO reactivity of Co(Por) modified electrodes was tested in both the Co(II) and Co(III) oxidation states by electrochemical methods. While $Co^{III}(Por)$ reacts efficiently with HNO, it does not so with NO. This is evidenced by the presence of the $[Co^{III}(Por)NO]^+/[Co^{II}(Por)NO]$ oxidation peak at 0.8 V, after HNO addition to the Co(Por) electrode, and the lack of any electrochemical signal when NO donors are used instead. On the contrary, NO reacts rapidly with $Co^{II}(Por)$ modified electrodes while HNO does not. In summary, Co(Por) attached to gold retains the same selective reactivity behavior towards HNO and NO, as observed in solution. Based on the redox dependent selective reactivity observed for the Co(Por) bound electrodes towards NO and HNO, and the redox potential shift due to a surface effect, reaction Scheme 8 was proposed to selectively detect HNO amperometrically. According to Scheme 8, the resting state electrode potential is set to 0.8 V, a value where the porphyrin is stable in the $Co^{III}(Por)$ state and no current flow is observed. Reaction with HNO yields, according to previous observations, the $Co^{III}(Por)NO^-$ complex, which under the described conditions is oxidized to $Co^{III}(Por)NO$. The resulting $Co^{III}(Por)NO$ complex releases the NO ligand in a fast manner and yields $Co^{III}(Por)$, which allows the catalytic cycle to start again. In this scheme the current intensity should be proportional to the amount of HNO that binds the $Co^{III}(Por)$. Consistent with the proposed scheme, measurement of the current vs. time plot at 0.8 V, where $Co^{III}(Por)$ is stable, does not show any measurable current change. However, a few seconds after the addition of AS the current intensity increases, and is maintained during several minutes, due

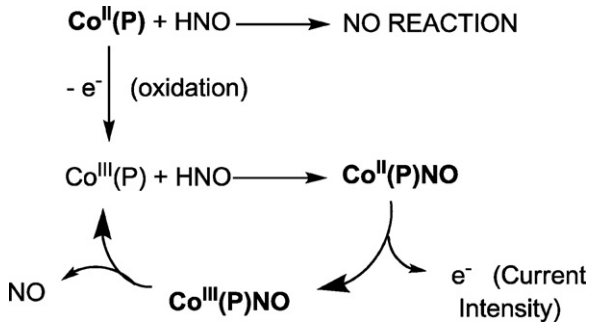

Scheme 8. Reactions involved in the amperometric detection of HNO by Co(Por) [157].

to the catalytic cycle, which is sustained by continuous HNO production from the donor, while no signal is produced by the addition of either NO(g) or NO donors. These results make a strong point for the use of Co^{III}(Por) electrodes as selective azanone sensors [157].

4. Summary, outlook and perspectives

4.1. What can we expect for in vivo HNO reactivity?

The comparative analysis of azanone reactivity with small molecules and proteins in the context of physiological systems strongly suggest that its main targets are constituted by thiols such as cysteine [103,179], and metalloproteins, mostly ferric heme proteins. Reaction with abundant oxygen is too slow to be important, and nitroxyl does not react with superoxide anion [40,112,180]. The reaction with thiols, from a protein cysteine residue, leads to reversible or irreversible modification of the corresponding protein [181]. The reaction can thus lead to protein inactivation, which depending on the protein could have beneficial or deleterious effects. In this context, more research is needed in order to understand: (i) which thiol-containing proteins are the preferred targets of HNO (or its donors); (ii) which are the particular microenvironmental characteristics of a given thiol (i.e. pK_a, hydrophobicity, solvent exposure, structural context) that determine and regulate its reactivity towards HNO; (iii) what are the results, in terms of chemical or protein postraductional modifications due to the reaction of nitroxyl with thiols in each particular case; and (iv) what is the consequence of HNO mediated Cysteine modification for the protein function.

Concerning the reaction with heme proteins, although stable complexes have been reported for ferrous myoglobin and other globins, it is still not clear if this reaction is physiologically relevant [95,125,126]. Moreover, kinetic studies related to the formation and decomposition of the corresponding complexes are needed in order to have a better estimation of their competing reactivity and stability. On the contrary, moderate to fast association rates, which results in a reductive nitrosylation that yields the quite stable ferrous nitrosyl complexes, characterizes the reaction of HNO with ferric heme proteins. The studied examples include several cytochromes and peroxidases [51,115,166,182,183]. The resulting complexes may be inactive for normal protein function providing an explanation for the observed HNO effects. Which specific protein is targeted will however depend on the local protein concentration and its specific reactivity, which in turns depends on the local environment of the heme, as for other ligands.

The possibly most important and relevant target of HNO *in vivo* is however the NO receptor soluble guanylate cyclase (sGC) [184,185]. The ferrous heme protein sGC becomes activated upon NO binding, increasing the cyclic GMP (cGMP) levels that trigger relaxation of vascular smooth muscle cells increasing the blood flow in small vessels [185,186]. The mechanism of signal transduction relies in the formation of an $\{FeNO\}^7$ adduct, which triggers proximal histidine release, due to the NO trans effect, and results in a conformational change that activates sGC [184–187]. Recently, HNO was shown to be capable of activating sGC [188]. This result is in contrast to previous studies that claimed that NO was the only nitrogen oxide capable of activating sGC [189]. The striking feature of the recent results is that, although HNO mediated sGC activation occurs via interaction with the heme, unexpectedly it does not activate the ferric form of the enzyme. In addition, in the corresponding work it was shown that higher HNO concentrations also lead to reaction with a cysteine leading to sGC inhibition [188]. Although HNO-mediated sGC activation is an appealing hypothesis, several points remain to be elucidated in order to establish it as a definite fact. Firstly, the reaction of HNO with both ferric and ferrous sGC must be studied in detail and its relation to sGC activity should be well defined. Secondly, the outcome of the reaction with cysteine needs to be addressed as well as the resulting effect on the sGC functionality. Finally, the reaction conditions should be carefully controlled to avoid possible conversion of HNO to NO leading to inconsistent results. *In any case, it can be accepted that thiol and heme containing proteins are the main physiological targets of HNO.*

4.2. Can we design a reliable, sensitive, selective and physiologically compatible HNO sensor?

Until recently, only indirect detection methods for HNO were available, the most popular being measurement of N_2O concentration [51,157]. Other methods relied in the use of thiols, and although they provide possible discrimination from NO [179], product purification and identification is required. The lack of accurate and reliable HNO detection and measurement methods, that are also able to discriminate HNO from NO and other interfering species, results in difficulties for: (i) assessing the reliability and optimal releasing conditions of HNO donors; (ii) unequivocal determination of the involvement of HNO in the previously described reactivity patterns under physiological-like conditions and most importantly (iii) determination of endogenous HNO production, as will be discussed below.

In the last few years, as described above, several methods have been developed to detect and quantify HNO in a reliable manner [157,167,170,171]. The presented methods either rely on optical (UV–vis, Fluorescence), spectroscopically (EPR) or electrochemical measurements [157]. UV–vis based methods, like manganese porphyrin based xerogels, have severe limitations for biological samples because the signal to be observed overlaps with the absorbance of heme proteins, which are the main targets under study. Also, they may interfere with the physiological state if used *in vivo*, since they react with several other targets besides HNO [116,190]. Fluorescence based methods, as developed by Lippard and coworkers [170,191,192], offer an interesting possibility, and are compatible with a cellular media, detecting HNO in a qualitative manner in the presence of NRS and ORS.

Metalloporphyrin modified electrodes that produce an electrochemical response to HNO offer an excellent prospect for the development of a reliable, sensitive, selective and physiologically compatible HNO sensor. Although clearly more work is needed in this area, present results indicate that HNO can be detected up to estimated concentrations of ca. 10 nM. This can be compared to the initial concentration of HNO produced by 10^{-3} M AS or PA in aerobic solutions at rt. and pH 7.4: ca. 100 nM. Moreover, the already studied Co-porphyrin modified electrode discriminates HNO from NO (i.e. it is completely insensitive to NO), and responds to repeated additions of an HNO donor, without signal loss [157]. What lies ahead is further development of this method in order to (i) test

the response in the presence of possible interfering species, like NO_2^-, O_2, O_2^-, $OONO^-$, NH_2OH, thiols, etc. (ii) calibrate the quantitative response to increasing HNO concentrations, (iii) improve the electrode by the use of nano-structured materials such as polyelectrolyte brushes [193] in order to increase the sensitivity to the pM level, and iv) achieve electrode miniaturization for *in vivo, in situ*, and inside-cell measurements. *In summary, a reliable, sensitive, selective and physiological compatible HNO sensing device should be available in the near future.*

4.3. Can we provide a definite answer to the endogenous HNO production paradox?

Given the unique biological properties described for HNO and the numerous *in vitro* assays suggesting the existence of several potential biosynthetic mechanisms for endogenous HNO production, it is tempting to envisage that this small molecule, like its cousin nitric oxide, could serve as an endogenous signaling molecule. The best candidates for endogenous HNO production are either the oxidation of hydroxylamine (or possibly hydroxyurea) by heme peroxidases [45], the conversion of NO to HNO by Mn or Fe superoxide dismutases [47] or by xanthine oxidase (XO) [194], or the production of HNO by NOS under certain special conditions [34,195]. From these options, the most reliable so far is the production of azanone by peroxidases, since its formation was evaluated with a recently developed selective assay in which the reaction products, $GS(O)NH_2$, in the presence of reduced glutathione (GSH) were quantified by HPLC [45]. Key for this reaction is the availability of active peroxidases and substrates *in vivo*. Also, further insights on the mechanism and the role played by the protein will contribute to clarify this matter. Concerning reduction of NO by SOD or XO, both studies relied on indirect methods for HNO detection which are sometimes difficult to interpret. Moreover, the low reduction potential of the $NO,H^+/^1HNO(^3NO^-)$ couple of ca. −0.55 to −0.8 V compared to 0.3 V for MnSOD makes NO reduction highly endergonic and unlikely. Clearly, the proposed HNO production by these enzymes has to be revised. Finally, HNO production by NOS also remains to be definitively proven, as the obtained evidence relies on the formation of $\{FeNO\}^7$ in the NOS active site, instead of the $\{FeNO\}^6$ species formed when NO is produced, or in the need for addition of Mn(III)SOD (that reduces HNO to NO) to the reacting media, to recover full NOS dependent sGC activation under low biopterin conditions [34,195]. In this context, a direct HNO detection method will surely contribute to definitely solve this issue.

However, the definitive proof for endogenous production of HNO in vivo, should be obtained by in situ measurements of HNO concentration in cell culture or tissues. A key element that will determine the possibility of performing such an experiment is the development of a biocompatible and selective HNO sensor.

Acknowledgements

This work was financially supported by the University of Buenos Aires UBACYT X065 and UBACyT2010-12ANPCyT (PICT 2006-2396 and PICT-07-1650) and CONICET PIP1207. MAM and FD are members of CONICET AL thanks Fulbright foundation for support via grant 49418515.

Appendix A. Supplementary data

Supplementary data associated with this article can be found, in the online version, at doi:10.1016/j.ccr.2011.04.012.

References

[1] H.W. Brown, G.C. Pimentel, J. Chem. Phys. 29 (1958) 883.
[2] G. Maier, H.P. Reisenauer, M. De Marco, Angew. Chem. Int. Ed. 38 (1999) 108–110.
[3] F. Dalby, J. Phys. 23 (1968) 136–143.
[4] P. Bruna, Chem. Phys. Lett. 67 (1979) 109–114.
[5] R. Guadagnini, G.C. Schatz, S.P. Walch, J. Chem. Phys. 102 (1995) 774.
[6] A. Luna, M. Merch, B. Srn, O. Roos, Chem. Phys. 196 (1995) 437–445.
[7] F.W. Dalby, Can. J. Phys. 36 (1958) 1336–1371.
[8] J.W.C. Johns, A.R.W. McKellar, J. Chem. Phys. 66 (1977) 1217.
[9] W. Anderson, Combust. Flame 117 (1999) 394–403.
[10] N.G. Connelly, T. Damhus, in: Nomenclature Of Inorganic Chemistry: IUPAC Recommendations 2005 (Red Book), Royal Society of Chemistry, 2005, p. 300.
[11] N.G. Connelly, T. Damhus, in: Nomenclature Of Inorganic Chemistry: IUPAC Recommendations 2005 (Red Book), Royal Society Of Chemistry, 2005, p. 98.
[12] N.G. Connelly, T. Damhus, in: Nomenclature Of Inorganic Chemistry: IUPAC Recommendations 2005 (Red Book), Royal Society Of Chemistry, 2005, p. 111.
[13] D. Parsonage, A.J. Greenfield, S.J. Ferguson, BBA-Bioenerget. 807 (1985) 81–95.
[14] V. Barone, Chem. Phys. Lett. 262 (1996) 201–206.
[15] V. Gutmann, H. Tannenberger, Monatsh. Chem. 87 (1956) 421–424.
[16] S. Moncada, R.M. Palmer, E.A. Higgs, Pharm. Rev. 43 (1991) 109–142.
[17] L.J. Ignarro, Kidney Int. 55 (1996) S2.
[18] K.M. Miranda, N. Paolocci, T. Katori, D.D. Thomas, E. Ford, M.D. Bartberger, M.G. Espey, D.A. Kass, M. Feelisch, J.M. Fukuto, D.A. Wink, Proc. Natl. Acad. Sci. 100 (2003) 9196–9201.
[19] N. Paolocci, W.F. Saavedra, K.M. Miranda, C. Martignani, T. Isoda, J.M. Hare, M.G. Espey, J.M. Fukuto, M. Feelisch, D.A. Wink, D.A. Kass, Proc. Natl. Acad. Sci. 98 (2001) 10463–10468.
[20] C.H. Switzer, W. Flores-Santana, D. Mancardi, S. Donzelli, D. Basudhar, L. a Ridnour, K.M. Miranda, J.M. Fukuto, N. Paolocci, D.A. Wink, Biochim. Biophys. Acta 1787 (2009) 835–840.
[21] E.C. DeMaster, F.N. Shirota, H.T. Nagasawa, Biochem. Biophys. Res. Commun. 122 (1984) 358–365.
[22] E. DeMaster, H. Nagasawa, F. Shirota, Pharmacol. Biochem. Behav. 18 (1983) 273–277.
[23] J.A. Reisz, E. Bechtold, S.B. King, Dalton Trans. (Cambridge, England: 2003) 39 (2010) 5203–5212.
[24] E.C. DeMaster, F.N. Shirota, H.T. Nagasawa, Alcohol 2 (1985) 117–121.
[25] E.G. DeMaster, B. Redfern, H.T. Nagasawa, Biochem. Pharm. 55 (1998) 2007–2015.
[26] S.I. Liochev, I. Fridovich, Free Radic. Biol. Med. 34 (2003) 1399–1404.
[27] J.M. Fukuto, R. Hszieh, P. Gulati, K.T. Chiang, H.T. Nagasaw, Biochem. Biophys. Res. Commun. 187 (1992) 1367–1373.
[28] J. Fukuto, P. Gulati, H.T. Nagasawa, Biochem. Pharm. 47 (1994) 922–924.
[29] A.J. Väänänen, P. Salmenperä, M. Hukkanen, P. Rauhala, E. Kankuri, Free Radic. Biol. Med. 41 (2006) 120–131.
[30] S. Lancel, J. Zhang, A. Evangelista, M.P. Trucillo, X. Tong, D.A. Siwik, R.A. Cohen, W.S. Colucci, Circ. Res. 104 (2009) 720–723.
[31] X.L. Ma, A.S. Weyrich, D.J. Lefer, A.M. Lefer, Circ. Res. 72 (1993) 403–412.
[32] O. Sidorkina, M.G. Espey, K.M. Miranda, D.A. Wink, J. Laval, Free Radic. Biol. Med. 35 (2003) 1431–1438.
[33] S. Adak, Q. Wang, D.J. Stuehr, J. Biol. Chem. 275 (2000) 33554–33561.
[34] H.H. Schmidt, H. Hofmann, U. Schindler, Z.S. Shutenko, D.D. Cunningham, M. Feelisch, Proc. Natl. Acad. Sci. 93 (1996) 14492–14497.
[35] M. Feelisch, M. Te Poel, R. Zamora, A. Deussen, S. Moncada, Nature 368 (1994) 62–65.
[36] Y. Ishimura, Y.T. Gao, S.P. Panda, L.J. Roman, B.S.S. Masters, S.T. Weintraub, Biochem. Biophys. Res. Commun. 338 (2005) 543–549.
[37] A.J. Hobbs, J.M. Fukuto, L.J. Ignarro, Proc. Natl. Acad. Sci. 91 (1994) 10992–10996.
[38] J.J. Woodward, Y. Nejatyjahromy, R.D. Britt, M.A. Marletta, Control (2010) 5105–5113.
[39] S. Stoll, Y. NejatyJahromy, J.J. Woodward, A. Ozarowski, M.A. Marletta, R.D. Britt, J. Am. Chem. Soc. 132 (2010) 11812–11823.
[40] K.M. Miranda, R.W. Nims, D.D. Thomas, M.G. Espey, D. Citrin, M.D. Bartberger, N. Paolocci, J.M. Fukuto, M. Feelisch, D.A. Wink, J. Inorg. Biochem. 93 (2003) 52–60.
[41] M.G. Espey, K.M. Miranda, D.D. Thomas, D.A. Wink, Free Radic. Biol. Med. 33 (2002) 827–834.
[42] S. Donzelli, M.G. Espey, D.D. Thomas, D. Mancardi, C.G. Tocchetti, L. a Ridnour, N. Paolocci, S.B. King, K.M. Miranda, G. Lazzarino, J.M. Fukuto, D.A. Wink, Free Radic. Biol. Med. 40 (2006) 1056–1066.
[43] D.A. Wink, J.A. Cook, S.Y. Kim, Y. Vodovotz, R. Pacelli, M.C. Krishna, J.B. a Russo, D. Mitchell, Jourdheuil, a M. Miles, M.B. Grisham, J. Biol. Chem. 272 (1997) 11147–11151.
[44] K.M. Miranda, A.S. Dutton, L. a Ridnour, C. a Foreman, E. Ford, N. Paolocci, T. Katori, C.G. Tocchetti, D. Mancardi, D.D. Thomas, M.G. Espey, K.N. Houk, J.M. Fukuto, D.A. Wink, J. Am. Chem. Soc. 127 (2005) 722–731.
[45] S. Donzelli, M.G. Espey, W. Flores-Santana, C.H. Switzer, G.C. Yeh, J. Huang, D.J. Stuehr, S.B. King, K.M. Miranda, D.A. Wink, Free Radic. Biol. Med. 45 (2008) 578–584.
[46] S.E. Bari, V.T. Amorebieta, M.M. Gutiérrez, J.A. Olabe, F. Doctorovich, J. Inorg. Biochem. 104 (2010) 30–36.
[47] V. Niketic, S. Stojanovic, A. Nikolic, A.M. Michelson, Free Radic. Biol. Med. 27 (1999) 992–996.

[48] D.R. Arnelle, J.S. Stamler, Arch. Biochem. Biophys. 318 (1995) 279–285.
[49] D.A. Stoyanovsky, Y.Y. Tyurina, V.A. Tyurin, D. Anand, D.N. Mandavia, D. Gius, J. Ivanova, B. Pitt, T.R. Billiar, V.E. Kagan, J. Am. Chem. Soc. 127 (2005) 15815–15823.
[50] K.M. Miranda, H.T. Nagasawa, J.P. Toscano, Curr. Top. Med. Chem. 5 (2005) 649–664.
[51] K.M. Miranda, Coord. Chem. Rev. 249 (2005) 433–455.
[52] A. Angeli, Gazz. Chim. Ital. 26 (1896) 17–25.
[53] A. Angeli, F. Angelico, Gazz. Chim. Ital. 33 (1903) 245.
[54] M.N. Hughes, P.E. Wimbledon, J. Chem. Soc. Dalton Trans. 8 (1976) 703–707.
[55] F. Bonner, B. Ravid, Inorg. Chem. 14 (1975) 558–563.
[56] J. Veprek-Siska, V. Pliska, F. Smirous, F. Visely, Collect. Czech. Chem. Commun. 24 (1959) 687–693.
[57] M.N. Hughes, P.E. Wimbledon, Chem. Ind. (1975) 742–743.
[58] C.M. Maragos, D. Morley, D.A. Wink, T.M. Dunams, J.E. Saavedra, A. Hoffman, A.A. Bove, L. Isaac, J.A. Hrabie, L.K. Keefer, J. Med. Chem. 34 (1991) 3242–3247.
[59] F.T. Bonner, B. Ravid, Inorg. Chem. 14 (1976) 548–553.
[60] O. Piloty, Ber. Dtsch. Ges. 29 (1896) 1559.
[61] P.C. Wilkins, H.K. Jacobs, M.D. Johnson, A.S. Gopalan, Inorg. Chem. 43 (2004) 7877–7881.
[62] M. Blackburn, B. Mann, B. Taylor, A. Worrall, Eur. J. Biochem./FEBS 153 (1985) 553.
[63] J. Scholz, P. Engel, C. Glidewell, K. Whitmire, Tetrahedron 45 (1989) 7695.
[64] A. Porcheddu, L. De Luca, G. Giacomelli, Synlett 2009 (2009) 2149–2153.
[65] A. Angeli, F. Angelico, F. Scurti, Chem. Central-Blatt. 73 (1902) 691–693.
[66] F.T. Bonner, Y.H. Ko, Inorg. Chem. 31 (1992) 2514–2519.
[67] F. Seel, C. Bliefert, Z. Anorg, Allg. Chem. 394 (1972) 187–196.
[68] R. Zamora, A. Grzesiok, H. Weber, M. Feelisch, Biochem. J. 312 (1995) 333.
[69] K.M. Miranda, T. Katori, C.L. Torres de Holding, L. Thomas, L. a Ridnour, W.J. McLendon, S.M. Cologna, A.S. Dutton, H.C. Champion, D. Mancardi, C.G. Tocchetti, J.E. Saavedra, L.K. Keefer, K.N. Houk, J.M. Fukuto, D.A. Kass, N. Paolocci, D.A. Wink, J. Med. Chem. 48 (2005) 8220–8228.
[70] S.V. Lymar, V. Shafirovich, J. Chem. Phys. B 111 (2007) 6861–6867.
[71] L. Keefer, R. Nims, K. Davies, D. Wink, Methods Enzymol. 268 (1996) 281.
[72] H. Nagasawa, E. DeMaster, B. Redfern, F. Shirota, D. Goon, J. Med. Chem. 33 (1990) 3120–3122.
[73] B.-B. Zeng, J. Huang, M.W. Wright, S.B. King, Bioorg. Med. Chem. Lett. 14 (2004) 5565–5568.
[74] S.B. King, Curr. Top. Med. Chem. 5 (2005) 665–673.
[75] X. Sha, T.S. Isbell, R.P. Patel, C.S. Day, S.B. King, J. Am. Chem. Soc. 128 (2006) 9687–9692.
[76] T.F. Emery, J. Neilands, J. Org. Chem. 27 (1962) 1075–1077.
[77] Y. Adachi, H. Nakagawa, K. Matsuo, T. Suzuki, N. Miyata, Chem. Commun. (2008) 5149–5151.
[78] K. Matsuo, H. Nakagawa, Y. Adachi, E. Kameda, H. Tsumoto, T. Suzuki, N. Miyata, Chem. Commun. (Cambridge, England) 46 (2010) 3788–3790.
[79] V. Shafirovich, S.V. Lymar, Proc. Natl. Acad. Sci. 99 (2002) 7340–7345.
[80] J.R. Buchholz, R.E. Powell, J. Am. Chem. Soc. 85 (1963) 509–511.
[81] S.V. Lymar, V. Shafirovich, G.A. Poskrebyshev, Inorg. Chem. 44 (2005) 5212–5221.
[82] S. Goldstein, G. Czapski, Free Radic. Biol. Med. 19 (1995) 505–510.
[83] R.E. Huie, S. Padmaja, Free Radic. Res. Commun. 18 (1993) 195–199.
[84] S. Goldstein, G. Czapski, J. Am. Chem. Soc. 118 (1996) 3419–3425.
[85] H.M. Smallwood, J. Am. Chem. Soc. 51 (1929) 1985–1999.
[86] S. King, H. Nagasawa, Methods Enzymol. 301 (1999) 211.
[87] L.E. Orgel, J. Chem. Soc. (Resumed) (1953) 1276.
[88] A.D. Walsh, J. Chem. Soc. (Resumed) (1953) 2288.
[89] M.D. Bartberger, W. Liu, E. Ford, K.M. Miranda, C. Switzer, J.M. Fukuto, P.J. Farmer, D.A. Wink, K.N. Houk, Proc. Natl. Acad. Sci. 99 (2002) 10958–10963.
[90] M. Tronc, A. Huetz, M. Landau, F. Pichou, J. Reinhardt, J. Phys. B: At. Mol. Phys. 8 (1975) 1160–1169.
[91] D. Teillet-Billy, F. Fiquet-Fayard, J. Phys. E: At. Mol. Phys. 10 (1977) Llll-7.
[92] C. Szmytkowski, K. Maciag, J. Phys. B: Atom. Mol. Phys. (1991) 4273.
[93] J. Tennyson, C. Noble, J. Phys. B: At. Mol. Phys. 19 (1986) 4025.
[94] A.C. Montenegro, V.T. Amorebieta, L.D. Slep, D.F. Martín, F. Roncaroli, D.H. Murgida, S.E. Bari, J.A. Olabe, Angew. Chem. Int. Ed. 48 (2009) 4213–4216.
[95] M.R. Kumar, J.M. Fukuto, K.M. Miranda, P.J. Farmer, Inorg. Chem. 49 (2010) 6283–6292.
[96] L. Cheng, G.B. Richter-Addo, in: K.M. Kadish, K. Smith, R. Guilard (Eds.), Academic Press, San Diego, 2000, pp. 219–291.
[97] F.C. Kohout, F.W. Lampe, J. Am. Chem. Soc. 87 (1965) 5795.
[98] P.A.S. Smith, G.E. Hein, J. Am. Chem. Soc. 82 (1960) 5731–5740.
[99] J.R. Buchholz, R.E. Powell, J. Am. Chem. Soc. 87 (1965) 2350–2353.
[100] F.T. Bonner, L.S. Dzelzkalns, J.A. Bonucci, Inorg. Chem. 17 (1978) 2487–2494.
[101] A.L. Smith, H.L. Johnston, J. Am. Chem. Soc. (1952) 12–14.
[102] M.G. Bryukov, A.A. Kachanov, R. Timonnen, J. Seetula, J. Vandoren, O.M. Sarkisov, Chem. Phys. Lett. 208 (1993) 392–398.
[103] M.D. Bartberger, J.M. Fukuto, K.N. Houk, Proc. Natl. Acad. Sci. 98 (2001) 2194–2198.
[104] P.C. Ford, Inorg. Chem. 49 (2010) 6226–6239.
[105] M. Hoshino, L. Laverman, P.C. Ford, Coord. Chem. Rev. 187 (1999) 75–102.
[106] K.M. Kadish, The Porphyrin Handbook, Academic Press, 2000.
[107] G.B. Richter-Addo, P. Legzdins, Metal Nitrosyls, Oxford University, New York, 1992.
[108] J.H. Enemark, R.D. Feltham, J. Am. Chem. Soc. 96 (1974) 5002–5004.
[109] B.L. Westcott, J.H. Enemark, Inorganic Electronic Structure and Spectroscopy, John Wiley & Sons, New York, 1999.
[110] J.H. Enemark, R.D. Feltham, Coord. Chem. Rev. 13 (1974) 339–406.
[111] G.R.A. Wyllie, W.R. Scheidt, Chem. Rev. 102 (2002) 1067–1090.
[112] J. Pellegrino, S.E. Bari, D.E. Bikiel, F. Doctorovich, J. Am. Chem. Soc. 132 (2010) 989–995.
[113] L.E. Laverman, P.C. Ford, J. Am. Chem. Soc. 123 (2001) 11614–11622.
[114] B.B. Wayland, L.W. Olson, J. Am. Chem. Soc. 96 (1974) 6037–6041.
[115] M. Hoshino, M. Maeda, R. Konishi, H. Seki, P.C. Ford, J. Am. Chem. Soc. 118 (1996) 5702–5707.
[116] I. Spasojevic, I. Batini-Haberle, I. Fridovich, Nitric Oxide 4 (2000) 526–533.
[117] Z.N. Zahran, J. Lee, S.S. Alguindigue, M.A. Khan, G.B. Richter-Addo, Dalton Trans. (Cambridge, England: 2003) (2004) 44–50.
[118] W.R. Scheidt, J.L. Hoard, J. Am. Chem. Soc. 95 (1973) 8281–8288.
[119] F. Roncaroli, R.V. Eldik, J. Am. Chem. Soc. 128 (2006) 8042–8053.
[120] M.P. Schopfer, J. Wang, K.D. Karlin, Inorg. Chem. 49 (2010) 6267–6282.
[121] M.R.A. Blomberg, P.E.M. Siegbahn, Biochim. Biophys. Acta 1757 (2006) 969–980.
[122] V.K.K. Praneeth, C. Näther, G. Peters, N. Lehnert, Inorg. Chem. 45 (2006) 2795–2811.
[123] J.P. Collman, A. Dey, Y. Yang, R.A. Decréau, T. Ohta, E.I. Solomon, J. Am. Chem. Soc. 130 (2008) 16498–16499.
[124] J.P. Collman, Y. Yang, A. Dey, R. a Decréau, S. Ghosh, T. Ohta, E.I. Solomon, Proc. Natl. Acad. Sci. 105 (2008) 15660–15665.
[125] F. Sulc, C.E. Immoos, D. Pervitsky, P.J. Farmer, J. Am. Chem. Soc. 126 (2004) 1096–1101.
[126] M.R. Kumar, D. Pervitsky, L. Chen, T. Poulos, S. Kundu, M.S. Hargrove, E.J. Rivera, A. Diaz, J.L. Colón, P.J. Farmer, Biochem 48 (2009) 5018–5025.
[127] D.A. Bazylinski, T.C. Hollocher, J. Am. Chem. Soc. 107 (1985) 7982–7986.
[128] S.E. Bari, M. a Martí, V.T. Amorebieta, D. a Estrin, F. Doctorovich, J. Am. Chem. Soc. 125 (2003) 15272–15273.
[129] M.A. Martí, S.E. Bari, D.A. Estrin, F. Doctorovich, J. Am. Chem. Soc. 127 (2005) 4680–4684.
[130] S.A. Suárez, M.A. Martí, P.M. De Biase, D.A. Estrin, S.E. Bari, F. Doctorovich, Polyhedron 26 (2007) 4673–4679.
[131] L.W. Olson, D. Schaeper, D. Lancon, K.M. Kadish, J. Am. Chem. Soc. 104 (1982) 2042–2044.
[132] D. Lancon, K.M. Kadish, J. Am. Chem. Soc. 105 (1983) 5610–5617.
[133] I.K. Choi, Y. Liu, D. Feng, K.J. Paeng, M.D. Ryan, Inorg. Chem. 30 (1991) 1832–1839.
[134] Z. Wei, M.D. Ryan, Inorg. Chem. 49 (2010) 6948–6954.
[135] M.H. Barley, K. Takeuchi, W.R. Murphy, T.J. Mayer, J. Chem. Soc., Chem. Commun. (1985) 507.
[136] J.N. Younathan, K.S. Wood, T.J. Meyer, Inorg. Chem. 31 (1992) 3280–3285.
[137] M.H. Barley, T.J. Meyer, J. Am. Chem. Soc. 108 (1986) 5876–5885.
[138] J. Lee, G.B. Richter-Addo, J. Inorg. Biochem. 98 (2004) 1247–1250.
[139] P.J. Farmer, F. Sulc, J. Inorg. Biochem. 99 (2005) 166–184.
[140] P.J. Farmer, M.R. Kumar, E. Almaraz, Comments Inorg. Chem. 31 (2010) 130–143.
[141] R.G. Serres, C.A. Grapperhaus, E. Bothe, E. Bill, T. Weyhermüller, F. Neese, K. Wieghardt, J. Am. Chem. Soc. 126 (2004) 5138–5153.
[142] J. Pellegrino, R. Hübner, F. Doctorovich, W. Kaim, Chem. Eur. J. (2011), doi:10.1002/chem.201003516.
[143] M. Graetzel, S. Taniguchi, A. Henglein, Berichte Der Bunsen-Gesellschaft Bot. Acta 74 (1970) 1003–1010.
[144] O. Einsle, A. Messerschmidt, P. Stach, G.P. Bourenkov, H.D. Bartunik, R. Huber, P.M. Kroneck, Nature 400 (1999) 476–480.
[145] O. Einsle, A. Messerschmidt, R. Huber, P.M.H. Kroneck, F. Neese, J. Am. Chem. Soc. 124 (2002) 11737–11745.
[146] N. Lehnert, V. Praneeth, F. Paulat, J. Comput. Chem. 27 (2006) 1338–1351.
[147] D.J. Richardson, N.J. Watmough, Curr. Opin. Chem. Biol. 3 (1999) 207–219.
[148] S.J. Ferguson, Curr. Opin. Chem. Biol. 2 (1998) 182–193.
[149] I. Moura, J.J. Moura, Curr. Opin. Chem. Biol. 5 (2001) 168–175.
[150] M. Fujii, J. Biol. Chem. 270 (1995) 1617–1623.
[151] E. Obayashi, S. Takahashi, Y. Shiro, J. Am. Chem. Soc. 120 (1998) 12964–12965.
[152] D.L. Harris, Int. J. Quantum Chem. 88 (2002) 183–200.
[153] A. Daiber, T. Nauser, N. Takaya, T. Kudo, P. Weber, C. Hultschig, H. Shoun, V. Ullrich, J. Inorg. Biochem. 88 (2002) 343–352.
[154] M. Vincent, I. Hillier, J. Ge, Chem. Phys. Lett. 407 (2005) 333–336.
[155] D.P. Linder, K.R. Rodgers, Inorg. Chem. 44 (2005) 8259–8264.
[156] Y. Ling, C. Mills, R. Weber, L. Yang, Y. Zhang, J. Am. Chem. Soc. 132 (2010) 1583–1591.
[157] S.A. Suárez, M.H. Fonticelli, A.A. Rubert, E. de La Llave, D. Scherlis, R.C. Salvarezza, M.A. Martí, F. Doctorovich, Inorg. Chem. 49 (2010) 6955–6966.
[158] D.G. Whitten, E.W. Baker, A.H. Corwin, J. Org. Chem. 28 (1963) 2363–2368.
[159] A.S. Dutton, J.M. Fukuto, K.N. Houk, J. Am. Chem. Soc. 126 (2004) 3795–3800.
[160] P.C. Wilkins, H.K. Jacobs, M.D. Johnson, A.S. Gopalan, Inorg. Chem. 43 (2004) 7877.
[161] W. Koppenol, J. Moreno, W.A. Pryor, H. Ischiropoulos, J. Beckman, Chem. Res. Toxicol. 5 (1992) 834–842.
[162] E.E. Scott, Q.H. Gibson, J.S. Olson, J. Biol. Chem. 276 (2001) 5177.
[163] V.S. Sharma, R.A. Isaacson, M.E. John, M.R. Waterman, M. Chevion, Biochem 22 (1983) 3897.
[164] M. Hoshino, F. Matsuzaki, Y. Nabeshima, C. Hama, Neuron 10 (1993) 395–407.
[165] L.E. Laverman, A. Wanat, J. Oszajca, G. Stochel, P.C. Ford, R. van Eldik, J. Am. Chem. Soc. 123 (2001) 285–293.

[166] I. Boron, S.A. Suárez, F. Doctorovich, M.A. Martí, S.E. Bari, J. Inorg. Biochem. 105 (2011) 1044–1049.
[167] K.P. Dobmeier, D.A. Riccio, M.H. Schoenfisch, Anal. Chem. 80 (2008) 1247–1254.
[168] D.W. Shoeman, H.T. Nagasawa, Nitric Oxide–Biol. Ch. 2 (1998) 66–72.
[169] K.M. Miranda, M.G. Espey, K. Yamada, M. Krishna, N. Ludwick, S.M. Kim, D. Jourd'heuil, M.B. Grisham, M. Feelisch, J.M. Fukuto, D.A. Wink, J. Biol. Chem. 276 (2001) 1720.
[170] A.G. Tennyson, L. Do, R.C. Smith, S.J. Lippard, Nitric Oxide 26 (2007) 4625–4630.
[171] J. Rosenthal, S.J. Lippard, J. Am. Chem. Soc. 132 (2010) 5536–5537.
[172] Y. Xia, A. Cardounel, A.F. Vanin, J.L. Zweier, Free Radic. Biol. Med. 29 (2000) 793–797.
[173] A. Komarov, Free Radic. Biol. Med. 28 (2000) 739–742.
[174] U. Samuni, Y. Samuni, S. Goldstein, J. Am. Chem. Soc. 132 (2010) 8428–8432.
[175] T. Akaike, M. Yoshida, Y. Miyamoto, K. Sato, M. Kohno, K. Sasamoto, K. Miyazaki, S. Ueda, H. Maeda, Biochem 32 (1993) 827–832.
[176] G. Guillaud, Coord. Chem. Rev. 178–180 (1998) 1433–1484.
[177] I.R. Davies, X. Zhang, Methods Enzymol. 436 (2008) 63–95.
[178] G.B. Richter-Addo, S.J. Hodge, G.B. Yi, M.A. Khan, T. Ma, E. Van Caemelbecke, N. Guo, K.M. Kadish, Inorg. Chem. 35 (1996) 6530–6538.
[179] S. Donzelli, M.G. Espey, D.D. Thomas, D. Mancardi, C.G. Tocchetti, L.A. Ridnour, N. Paolocci, S.B. King, K.M. Miranda, G. Lazzarino, J.M. Fukuto, D.A. Wink, Free Radic. Biol. Med. 40 (2006) 1056–1066.
[180] J.C. Irvine, R.H. Ritchie, J.L. Favaloro, K.L. Andrews, R.E. Widdop, B.K. Kemp-Harper, Trends Pharmacol. Sci. 29 (2008) 601–608.
[181] B. Shen, A.M. English, Biochem 44 (2005) 14030–14044.
[182] D.E. Bikiel, L. Boechi, L. Capece, A. Crespo, P.M. De Biase, S. Di Lella, M.C. González Lebrero, M.A. Martí, A.D. Nadra, L.L. Perissinotti, D.A. Scherlis, D.A. Estrin, Phys. Chem. Chem. Phys.: PCCP 8 (2006) 5611–5628.
[183] M.P. Doyle, S.N. Mahapatro, R.D. Broene, J.K. Guy, J. Am. Chem. Soc. 110 (1988) 593–599.
[184] J.W. Denninger, M.A. Marletta, BBA-Bioenerget. 1411 (1999) 334–350.
[185] T.L. Poulos, Curr. Opin. Struct. Biol. 16 (2006) 736–743.
[186] A.J. Hobbs, L.J. Ignarro, Methods Enzymol. 269 (1996) 1996–11996.
[187] L. Capece, D.A. Estrin, M.A. Marti, Biochemistry 47 (2008) 9416–9427.
[188] T.W. Miller, M.M. Cherney, A.J. Lee, N.E. Francoleon, P.J. Farmer, S.B. King, A.J. Hobbs, K.M. Miranda, J.N. Burstyn, J.M. Fukuto, J. Biol. Chem. 284 (2009) 21788–21796.
[189] E.A. Dierks, J.N. Burstyn, Biochem. Pharm. 51 (1996) 1593–1600.
[190] I. Batinic-Haberle, I. Spasojevic, P. Hambright, L. Benov, A.L. Crumbliss, I. Fridovich, Inorg. Chem. 38 (1999) 4011–4022.
[191] M.H. Lim, S.J. Lippard, Nitric Oxide 43 (2004) 2071–2075.
[192] L.E. McQuade, S.J. Lippard, Curr. Opin. Chem. Biol. 14 (2010) 43–49.
[193] E.-Y. Choi, O. Azzaroni, N. Cheng, F. Zhou, T. Kelby, W.T.S. Huck, Langmuir 23 (2007) 10389–10394.
[194] M. Saleem, H. Ohshima, Biochem. Biophys. Res. Commun. 315 (2004) 455–462.
[195] J.J. Woodward, Y. Nejatyjahromy, R.D. Britt, M.A. Marletta, J. Am. Chem. Soc. 132 (2010) 5105–5113.
[196] R. Lin, P.J. Farmer, J. Am. Chem. Soc. 122 (2000) 2393–2394.
[197] C.E. Immoos, F. Sulc, P.J. Farmer, K. Czarnecki, D.F. Bocian, A. Levina, J.B. Aitken, R.S. Armstrong, P. Lay, J. Am. Chem. Soc. 127 (2005) 814–815.